1

Molecular Vibrational Motion

The atoms in matter – be it in gaseous, liquid, or condensed phases – are in constant motion. The amplitude of this motion increases with increasing temperature; however, even at absolute zero temperature, it never approaches zero or perfect stillness. Furthermore, the amplitude of the atomic motion is a measure of the thermodynamic heat content as measured by the product of the specific heat times the absolute temperature. If one could observe the motion in real time – which is not possible because the motions occur at a timescale of about 10^{13} Hz – one would find that it is completely random and that the atoms are most likely to be found in ellipsoidal regions in space, such as the ones depicted in X-ray crystallographic structures. Yet, the random motion can be decomposed into distinct "normal modes of vibration." These normal modes can be derived from classical physical principles (see Section 1.2) and are defined as follows: in a normal mode, all atoms vibrate, or oscillate, at the same frequency and phase, but with different amplitudes, to produce motions that are referred as symmetric and antisymmetric stretching, deformation, twisting modes, and so on. In general, a molecule with N atoms will have $3N-6$ normal modes of vibrational normal modes.

At this point, a discrepancy arises between the classical (Newtonian) description of the motion of atoms in a molecule and the quantum mechanical description. While in the classical description the amplitude of the motion, and thereby the kinetic energy of the moving atoms, can increase in arbitrarily small increments, the quantum mechanical description predicts that the increase in energy is quantized, and that infrared (IR) photons can be absorbed by a vibrating molecular system to increase the energy along one of the normal modes of vibration.

In the discussion to follow, the concepts of normal modes of vibration will be introduced for a system of spring-coupled masses, as shown in Figure 1.1, a typical mechanical model for a molecular system. Through a series of mathematical steps, the principle of normal modes will be derived from Newtonian laws of motion. Once this set of "normal modes" is defined, it is relatively trivial to extend these coordinates to a quantum mechanical description that results in the basic formalism for stationary vibrational states in molecules, and the transitions between these stationary states that are observed in IR and Raman spectroscopies.

Sections 1.1–1.7 are aimed at presenting a summary of the physical principles required for understanding the principles of vibrational spectroscopy. They do not present the subject with the mathematical rigor presented in earlier treatments, for example, in Wilson *et al.* [1] for the classical description of normal modes nor the quantum mechanical detail found in typical texts such as those by Kauzman [2] or Levine [3]. However, sufficient detail is provided to expose the reader to the necessary physical principles such as normal modes

Modern Vibrational Spectroscopy and Micro-Spectroscopy: Theory, Instrumentation and Biomedical Applications, First Edition.
Max Diem.

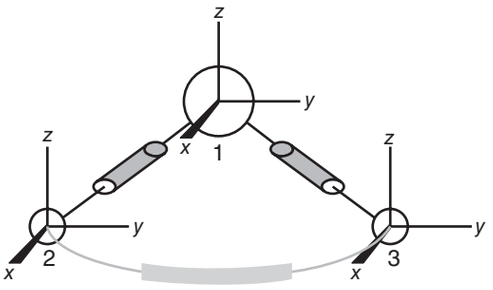

Figure 1.1 *"Mass-and-spring" model of Cartesian displacement vectors for a triatomic molecule. The gray cylinders represent springs obeying Hook's law*

of vibration and normal coordinates, the basic quantum mechanics of vibrating systems, and the transition moment, but in addition to the aforementioned texts, it will introduce the reader to many practical aspects of vibrational spectroscopy, as well as branches of vibrational spectroscopy that were not included in the earlier treatments.

For the remainder of this book, a standard convention for expressing vibrational energies in wavenumber units will be followed. Although energies should be expressed in units of Joule ($1\,\mathrm{J} = \mathrm{kg\,m^2\,s^{-2}}$), these numbers are unyielding, and wavenumber units are used throughout. The following energy unit conversions apply:

$$E = h\nu = \frac{hc}{\lambda} = h\,c\tilde{\nu}$$

Here, h has the value of $6.6 \times 10^{-34}\,\mathrm{J\,s}$. Using $h\nu = hc\tilde{\nu}$, one finds that $1\,\mathrm{cm^{-1}} \approx 30\,\mathrm{GHz} = 2 \times 10^{-23}\,\mathrm{J}$ (see also the table in the introduction and comments after Eqs. 1.31 and 1.63). Herewith, the author categorically apologizes for referring to transitions, expressed in wavenumber units, as "energies."

1.1 The concept of normal modes of vibration

Consider a set of masses connected by springs that obey Hook's law, as shown in Figure 1.1. Two of these springs act as restoring force when the "bonds" between atoms 1 and 2 and between atoms 1 and 3 are elongated or compressed, whereas one spring acts to restore the bond angle between atoms 2–1–3. Furthermore, we assume that the force required to move one atom along a coordinate depends on the momentary position of all other atoms: the force required to extend bond 1–2 may decrease if bond 1–3 is elongated. In a mechanical system, this situation is referred to as a coupled spring ensemble, where the stiffness of a spring depends on all coordinates. In a molecular system, this corresponds to electron rearrangement when the molecular shape changes, with a concomitant change in bond strength. In order to describe the atomic motions in a vibrating system, one attaches a system of Cartesian displacement coordinates to every atom, as shown in Figure 1.1. A normal mode of vibration then can be described as a combination of properly scaled displacement vector components.

1.2 The separation of vibrational, translational, and rotational coordinates

Based on Figure 1.1, one may expect a system of N atoms to exhibit $3N$ degrees of vibrational freedom: a degree of freedom for all three Cartesian displacement coordinates of each atom, or any linear combinations

of them. However, vibrational spectroscopy depends on a restoring force to bring the atoms of a molecule back to their equilibrium position. If, for example, all atoms in a molecule move simultaneously in the x-direction, by the same amount, no bonds are being compressed or elongated. Thus, this motion is not that of an internal vibrational coordinate but that of a translation. There are three translational degrees of freedom, corresponding to a motion of all atoms along the x, y, or z axes by the same amount. Another view of the same fact is that these modes have zero frequencies as there is no restoring force acting during the atomic displacements. This view will be favored in the derivation of the concepts of normal modes presented in Section 1.3, which is carried out in (mass-weighted) Cartesian displacement coordinates. Later on, a different and simpler coordinate system will be introduced as well.

Similarly, one can argue that certain combinations of Cartesian displacements correspond to a rotation of the entire molecule, where there is no change in the intermolecular potential of the atoms. There are three degrees of rotational freedom of a molecule, corresponding to rotations about the three axes of inertia. Subtracting these from the remaining number of degrees of freedom, one arrives at $3N-6$ degrees of vibrational freedom for a polyatomic, nonlinear molecule. Linear molecules have one more $(3N-5)$ degree of vibrational freedom, because they have only two moments of inertia. This is because one assumes a zero moment of inertia for a rotation about the longitudinal axis.

Mathematically, the separation of rotation and translation from the vibration of a molecule proceeds as follows: in order for the translational energy of the molecule to be zero at all times, one defines a coordinate system that translates with the molecule. In this coordinate system, the translational energy is zero by definition. The translating coordinate system is defined such that the center of mass of the molecule is at the origin of the coordinate system at all times. This leads to the condition

$$\sum_{\alpha=1}^{N} m_\alpha \xi_\alpha = 0 \tag{1.1}$$

where ξ denotes the X, Y, and Z coordinates of the α'th atom of a molecule with N atoms. Similarly, the rotational energy can be reduced to zero by defining a coordinate system that rotates with the molecule. This requires that the angular moments of the molecule in the rotating coordinate frame are zero, which leads to three more equations of zero frequencies. These six equations are needed to define a coordinate system in which both translational and rotational energies are zero. Details of this derivation can be found in Wilson *et al.* [1, Chapters 2 and 11].

1.3 Classical vibrations in mass-weighted Cartesian displacement coordinates

The concept of normal modes of vibration, necessary for understanding the quantum mechanical description of vibrational spectroscopy and obtaining a pictorial description of the atomic motions, can be introduced by the previously described classical model of a molecule consisting of a number of point masses, held in their equilibrium positions by springs. This kind of discussion is treated in complete detail in the classic books on vibrational spectroscopy, for example, in Chapter 2 of Wilson *et al.* [1].

The treatment starts with Lagrange's equation of motion:

$$\frac{d}{dt}\frac{\partial T}{\partial \dot{x}_i} + \frac{\partial V}{\partial x_i} = 0 \tag{1.2}$$

where T and V are the kinetic and potential energies, respectively, the x_i are the Cartesian displacement coordinates, and the dot denotes the derivative with respect to time. Equation 1.2 is another statement of Newton's equation of motion (Eq. 1.3) expressed in terms of the kinetic and potential energies, rather than terms of force and acceleration:

$$F_i = m_i \frac{d^2 x_i}{dt^2} \tag{1.3}$$

In Eq. 1.3, F represents the force, which is related to the potential energy by

$$F_i = -\frac{dV}{dx_i} = kx_i \tag{1.4}$$

Equation 1.4 is Hook's law, which states that the force F needed to elongate or compress a spring depends on the spring's stiffness, expressed by the force constant k, multiplied by the elongation of the spring, x. The acceleration (d^2x_i/dt^2) in Eq. 1.3 can be related to the kinetic energy as follows:

$$T = \frac{1}{2}\left(\sum_i m_i \dot{x}_i^2\right) \tag{1.5}$$

Thus,

$$\frac{dT}{d\dot{x}_i} = m_i \dot{x}_i \tag{1.6}$$

Substituting Eqs. 1.4 and 1.6 into Eq. 1.3 yields Lagrange's equation of motion in which the expressions for kinetic and potential energies appear separately. This formulation is advantageous for writing the quantum mechanical Hamiltonian, *cf.* the following section.

Next, one rewrites Eq. 1.2 in terms of mass-weighted displacement coordinates, q_i. The reason for this is that the amplitude of a particle's oscillation depends on its mass. When mass-weighted coordinates are used, all amplitudes are properly adjusted for the different masses of the particles. In addition, the use of mass-weighted coordinates simplifies the formalism quite a bit. Let

$$q_i = \sqrt{m_i} x_i \tag{1.7}$$

Then, the kinetic energy can be written as

$$2T = \sum_i^{3N} (\dot{q}_i)^2 \tag{1.8}$$

Note that Eq. 1.8 contains only "diagonal terms"; that is, no cross terms q_{ij} appear in the summation. (The term "diagonal" here refers to a matrix notation to be introduced shortly.) Next, the potential energy of the particles needs to be defined. For masses connected by springs obeying Hook's law, one may assume that the potential energy along each Cartesian displacement coordinate is given by

$$V = \frac{1}{2}\sum_{i=1}^{3N}\sum_{j=1}^{3N}\left(\frac{\partial^2 V}{\partial q_i \partial q_j}\right) dq_i dq_j \tag{1.9}$$

or

$$V = \frac{1}{2}\sum_{i=1}^{3N}\sum_{j=1}^{3N} f_{ij} dq_i dq_j \tag{1.10}$$

with

$$f_{ij} = \left(\frac{\partial^2 V}{\partial q_i \partial q_j}\right) \tag{1.11}$$

The f_{ij} are known as mass-weighted Cartesian force constants and differ from the force constant k defined in Eq. 1.4 by the fact that latter does not explicitly contain the masses of the atoms. The constants f_{ij} express the change in potential energy as an atom or group is moved along the directions given by q_i and q_j. For small displacements about the equilibrium positions, Eq. 1.10 can be written as

$$2V = \sum_{i=1}^{3N}\sum_{j=1}^{3N} f_{ij}\, q_i q_j \tag{1.12}$$

In contrast to the kinetic energy expression in mass-weighted Cartesian coordinates (Eq. 1.8), the potential energy depends on diagonal ($f_{ii}{q_i}^2$) and off-diagonal ($f_{ij}q_iq_j$) terms as pointed out earlier. Taking the required

derivatives and substituting the expressions for $\frac{d}{dt}\frac{\partial T}{\partial \dot{q}_i}$ and $\frac{\partial V}{\partial q_i}$ into Lagrange's equation of motion (Eq. 1.2) yields

$$\ddot{q}_i + \sum_{j=1}^{3N} f_{ij}\, q_j = 0 \tag{1.13}$$

Here, $\ddot{q}$ denotes the second derivative of q with respect to time. Equation 1.13 is a short form for a set of $3N$ simultaneous differential equations, with the index i running from 1 to $3N$. Note that the double summation in Eq. 1.12 disappears when the derivative with respect to one of the displacements, $\partial V/\partial q_i$, is taken. In expanded form, Eq. 1.13 can be presented as:

$$\begin{aligned}
\frac{d^2q_1}{dt^2} + f_{11}q_1 + f_{12}q_2 + f_{13}q_3 + \cdots + f_{1,3N}q_{3N} = 0 \\
\frac{d^2q_2}{dt^2} + f_{21}q_1 + f_{22}q_2 + f_{23}q_3 + \cdots + f_{2,3N}q_{3N} = 0 \\
\frac{d^2q_{3N}}{dt^2} + f_{3N,1}q_1 + f_{3N,2}q_2 + f_{3N,3}q_3 + \cdots + f_{3N,3N}q_{3N} = 0
\end{aligned} \tag{1.14}$$

In each equation, only one term in the summation $\sum f_{ij}q_j$ has the same index as the term containing the time derivative. Thus, these equations can be simplified to read

$$\ddot{q}_i + f_{ii}q_i + C = 0 \tag{1.15}$$

where C is a constant. There are $3N$ solutions to these simultaneous, linear differential equations:

$$q_i = A_i \sin(\sqrt{\lambda}t + \varepsilon) \tag{1.16}$$

where the A_i are amplitude factors, ε are phase angles, and λ is a quantity related to the frequency and determined by the force constants (*cf.* below). Following standard practice in solving linear differential equations, one takes the solution given by Eq. 1.16, differentiates twice with respect to time,

$$\frac{d^2q_i}{dt^2} = -\lambda q_i \tag{1.17}$$

and substitutes Eq. 1.15 back into Eq. 1.14. One obtains, after canceling the terms $\sin(\sqrt{\lambda}t + \varepsilon)$ from each equation:

$$\begin{aligned}
-A_1\lambda + f_{11}A_1 + f_{12}A_2 + f_{13}A_3 + \cdots + f_{1,3N}A_{3N} = 0 \\
f_{21}A_1 - A_2\lambda + f_{22}A_2 + f_{23}A_3 + \cdots + f_{2,3N}A_{3N} = 0 \\
f_{31}A_1 + f_{32}A_2 - A_3\lambda + f_{33}A_3 + \cdots + f_{3,3N}A_{3N} = 0 \\
\cdots
\end{aligned} \tag{1.18}$$

or

$$\begin{aligned}
(f_{11} - \lambda)A_1 + f_{12}A_2 + f_{13}A_3 + \cdots + f_{1,3N}A_{3N} = 0 \\
f_{21}A_1 + (f_{22} - \lambda)A_2 + f_{23}A_3 + \cdots + f_{2,3N}A_{3N} = 0 \\
f_{31}A_1 + f_{32}A_2 + (f_{33} - \lambda)A_3 + \cdots + f_{3,3N}A_{3N} = 0 \\
\cdots
\end{aligned} \tag{1.19}$$

Thus, $3N$ simultaneous homogeneous linear equations were obtained from $3N$ simultaneous linear differential equations. Homogeneous equations have two kinds of solutions. One of them is the so-called trivial solution in which all coefficient A_i are zero. This condition indeed fulfills Eq. 1.19 but is of no interest here because it implies that all particles are at rest; that is, there is no vibrational motion at all. The other solution for Eq. 1.19 is obtained when the determinant of the coefficients of A is zero in order for the left-hand side of Eq. 1.19 to be zero:

$$| (f_{ij} - \delta_{ij}\lambda) | = 0 \tag{1.20}$$

This is called the nontrivial solution, which requires

$$\begin{aligned} f_{11} - \lambda + f_{12} + f_{13} + \cdots + f_{1,3N} &= 0 \\ f_{21} + f_{22} - \lambda + f_{23} + \cdots + f_{2,3N} &= 0 \\ f_{31} + f_{32} + f_{33} - \lambda + \cdots + f_{3,3N} &= 0 \\ \cdots & \end{aligned} \tag{1.21}$$

Equation 1.21 is known as the vibrational secular equation. The solution of this equation gives the eigenvalues λ, which are related to the vibrational frequencies for each of the normal modes. The amplitude factors A_i in Eq. 1.19 are not determined, but the relative magnitude of the displacement vectors can provide a view of the relative amplitudes of all atoms during a normal mode of vibration.

A normal mode of vibration is defined to by one of the $3N$ solutions of Eq. 1.21, where all atoms oscillate with the same frequency and in-phase but with different amplitudes. This definition is one of the most important ones in vibrational spectroscopy. It implies that all atoms are in motion during a normal mode of vibration, which is required to maintain the center of mass of the molecule. If $3N$ mass-weighted Cartesian displacement coordinates are defined, six rotational and translational modes will appear in these calculations as eigenvalues with zero frequencies, as discussed earlier. The displacement vectors will confirm that these motions are, indeed, translations and rotations.

Before continuing the discussion of the normal modes in polyatomic molecules, the simpler case of the vibration of diatomic molecules will be presented. For a diatomic molecule (which, of course, must be linear), Eq. 1.21 described a set of six equations, five of which have zero frequencies (namely the three translational and the two rotational coordinates). That leaves one equation,

$$f_{11} - \lambda = 0 \tag{1.22}$$

or $\lambda = f_{11}$. Next, it is instructive to visualize that Eq. 1.22 actually represents a vibrational frequency. For a diatomic molecule, the vibrational frequency can also be derived, starting with Newton's second law,

$$F = m \frac{d^2 x}{dt^2} \tag{1.3}$$

and assuming a harmonic restoring force obeying Hook's law:

$$F = -kx \tag{1.23}$$

Thus, one can write the equation of motion for a diatomic molecule as

$$\frac{d^2x}{dt^2} + \frac{k}{m} x = 0 \tag{1.24}$$

Here, k is the spring's (bond's) force constant, as discussed earlier (Eq. 1.4) that corresponds to the terms f_{ij} in Eq. 1.19, and m is the reduced mass defined as

$$m = \frac{m_1 m_2}{m_1 + m_2} \tag{1.25}$$

with m_1 and m_2 the individual masses of the two atoms.

One valid solution of the differential equation of motion (Eq. 1.24) is

$$x(t) = A\ \sin(\omega t + \ \varepsilon) \tag{1.26}$$

where

$$\omega = 2\pi = \sqrt{\frac{k}{m}} \tag{1.27}$$

where ω is the angular frequency and ε is a phase angle. Note that for a classical vibrational problem, the amplitude A is arbitrary, but that the frequency is defined by Eq. 1.25. This implies that for larger amplitudes, the velocity of the motion of the particles increases, but the frequency remains constant.

Rewriting Eq. 1.27 as

$$k = m\omega^2 \tag{1.28}$$

and comparing Eqs. 1.22 and 1.28, one finds that

$$\sqrt{\lambda} = \ \omega \tag{1.29}$$

when using mass-weighted Cartesian displacement coordinates. This relationship is true for diatomic and polyatomic molecules. At this point, a quick analysis of magnitudes and units is appropriate. The force constant k acting in a diatomic molecule such as gaseous H—Cl typically is about $500\,\mathrm{N\,m^{-1}} = 500\,\mathrm{kg\,s^{-2}}$, corresponding to a relatively stiff spring in classical mechanics. The reduced mass of an H—Cl molecule is, according to Eq. 1.25, approximately

$$m = 1.56 \times 10^{-27}\ \mathrm{kg} \tag{1.30}$$

and thus, the vibrational frequency for the H—Cl molecule is found to be

$$\begin{aligned} \nu = \frac{1}{2\pi}\sqrt{\frac{k}{m}} = \ \frac{1}{2\pi}\sqrt{\frac{5.0\ \times 10^2}{1.56\ \times 10^{-27}}} = \frac{1}{2\pi}\,5.67 \times 10^{14} \\ = 9.0 \times 10^{13}((\mathrm{kg\ s^{-2}})/\mathrm{kg})^{1/2} = \mathrm{Hz} \end{aligned} \tag{1.31}$$

Using the frequency/wavenumber conversion $c\tilde{\nu} = \nu$ gives a value close to the observed stretching frequency for gaseous H—Cl of $3 \times 10^3\ \mathrm{cm^{-1}}$. When working in mass-weighted Cartesian displacement coordinates, the reduced mass in Eq. 1.27 disappears, and the frequency of the vibration is given by

$$\omega = \sqrt{\lambda} = \sqrt{f_{11}} \quad \text{or} \quad \nu = \frac{\sqrt{\lambda}}{2\pi} \tag{1.32}$$

Thus, Eq. 1.22, indeed, denotes the vibrational frequency of diatomic or polyatomic molecules.

Returning to the secular equation 1.21 for a triatomic molecule, one finds that one needs 81 force constants to describe the problem. Of these 81 force constants, only 9 are nonzero, because there are $3N-6$, or 3 degrees of vibrational freedom. However, it is clear that even this reduced problem cannot be solved,

because there are three equations with nine unknowns. Symmetry arguments reduce this number of unknown force constants even further, but the number of unknowns still exceeds the number of equations. In the past, this problem was alleviated by transferring the diagonal force constants, that is, those with common indexes (f_{ii}) from similar molecules or from isotopic species, assuming that the diagonal force constants should not depend on isotopic substitution. Off-diagonal force constants were fitted to reproduce observed frequencies. More recently, all force constants – diagonal and off-diagonal – are determined computationally *via ab initio* methods (*cf.* Chapter 6). However, the meaning of the off-diagonal force constants needs to be pointed out in more detail. Referring to Figure 1.1, the diagonal force constants f_{11}, f_{22}, and f_{33} refer to the force required to move atom 1 in the x, y, and z directions, respectively. The off-diagonal constant f_{12} describes the force required to move atom 1 in the y direction after displacement in the x-direction.

To obtain vibrational frequencies and a depiction of the normal modes, the system of simultaneous homogeneous linear equations (Eq. 1.21) needs to be solved. As described earlier, values for force constants are substituted into the force constant matrix (also referred to potential energy matrix) that is subsequently diagonalized numerically according to:

$$\mathbf{L}^{\mathbf{T}}\,\boldsymbol{F}\,\mathbf{L} = \Lambda \tag{1.33}$$

Here, the matrix $\boldsymbol{F}$ corresponds to the Cartesian force constant defined in Eq. 1.21, and the eigenvector matrix $\boldsymbol{L}$ that diagonalizes the potential energy matrix is also the matrix that transforms from the mass-weighted Cartesian coordinate system to a new coordinate system Q, known as the "normal coordinates." These normal coordinates are defined such that each of the $3N-6$ normal modes of vibration is associated with one and only one normal coordinate Q. For the discussion of the relationship between mass-weighted displacement coordinates q and the normal coordinates Q, it is advantageous to cast the previously obtained equations into matrix notation. In the following discussion, bold quantities imply matrices or vectors. The two relationships derived earlier, expressing the potential and kinetic energies in terms of mass-weighted Cartesian coordinates, are written in matrix notations as

$$2T = \sum_{i}^{3N} (\dot{q}_i)^2 \quad \text{or} \quad 2\mathbf{T} = \dot{\mathbf{q}}^{\mathbf{T}}\dot{\mathbf{q}} \tag{1.8}$$

and

$$2V = \sum_{i=1}^{3N}\sum_{j=1}^{3N} f_{ij}\,q_i q_j \quad \text{or} \quad 2\mathbf{V} = \mathbf{q}^{\mathbf{T}}\,\boldsymbol{F}\mathbf{q} \tag{1.12}$$

Here, the superscript $\mathbf{T}$ denotes the transpose of a matrix; thus, the column vector $\dot{\mathbf{q}}$ becomes a row vector upon transposition. The dot implies, as before, the time derivative of the coordinates. $\boldsymbol{F}$ denotes the matrix of mass-weighted Cartesian force constants, as defined in Eq. 1.33.

Normal coordinates are defined such that

$$2\mathbf{T} = \dot{\mathbf{Q}}^{\mathbf{T}}\,\dot{\mathbf{Q}}$$

$$\text{and} \quad 2\mathbf{V} = \mathbf{Q}^{\mathbf{T}}\Lambda\mathbf{Q} \tag{1.34}$$

In normal coordinate space, both the kinetic and potential energy matrices are diagonal. As the kinetic energy is diagonal in both q and Q space, the problem simplifies to finding the transformation (eigenvector) matrix $\boldsymbol{L}$ that diagonalizes the potential energy matrix $\boldsymbol{F}$. This matrix also transforms from the mass-weighted Cartesian displacement space into normal coordinate space according to

$$\mathbf{Q} = \mathbf{L}\,\mathbf{q} \tag{1.35}$$

Thus, the diagonalization of the potential energy matrix provides the vibrational frequencies of the system, according to

$$\omega_k = \sqrt{\lambda_k} \tag{1.36}$$

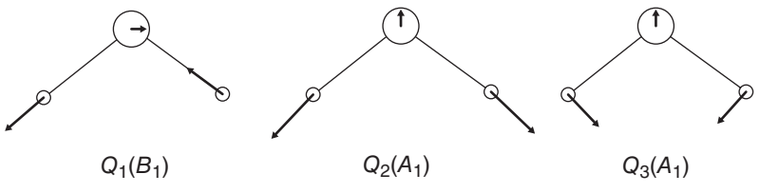

Figure 1.2 *Display of the atomic displacement vectors and the symmetries (see Chapter 2) for the three normal modes of the water molecule. The magnitude of the displacement vectors is not known, but the relative displacements are drawn approximately to scale. The terms A1, and B1 refer to the symmetry species of the coordinates (see Chapter 2).*

as well as the transformation to visualize each normal mode of vibration in terms of a normal coordinate and therewith, in terms of the displacement vectors. The displacement vectors for the normal modes of vibration of the water molecule are shown in Figure 1.2.

1.4 Quantum mechanical description of molecular vibrations

1.4.1 Transition from classical to quantum mechanical description

Next, a connection between the classical normal mode picture and the quantum mechanical description will be presented. The approach here starts with a simple case of a diatomic molecule for which the classical equation of motion was derived earlier (Eqs. 1.23–1.27) and for which the solution of the Schrödinger equation is relatively straightforward. Once the (one-dimensional) situation of the diatomic molecule has been introduced, the transition to polyatomic molecules is fairly simple because the concept of the normal coordinates can be used. As pointed out earlier, the classical description of the vibrations of a diatomic or polyatomic molecule predicts the vibrational coordinates (the normal modes) and their frequency, but not the transitions that are observed in IR absorption or Raman spectroscopy. In order to explain the observed spectra, quantum mechanics has to be invoked.

Quantum mechanics presents an approach to the behavior of microscopic particles very different from that in classical mechanics. While, in classical mechanics, the position and momentum of a moving particle can be established simultaneously, Heisenberg's uncertainty principle prohibits the simultaneous determination of those two quantities. This is manifested by Eq. 1.37 for the one-dimensional case:

$$\Delta p_x \Delta x \geq \frac{\hbar}{2} \tag{1.37}$$

which implies that the uncertainty in the momentum and position always exceeds $\hbar/2$. Mathematically, Eq. 1.37 follows from the fact that the operators responsible for defining position and momentum, $\hat{x}$ and $\hat{p}_x$, do not commutate; that is, $[\hat{x}, \hat{p}_x] \neq 0$. The incorporation of this uncertainty into the picture of the motion of microscopic particles leads to discrepancies between classical and quantum mechanics: classical physics has a deterministic outcome, which implies that if the position and velocity (trajectory) of a moving body are established, and it is possible to predict with certainty where it is going to be found in the future. Quantum mechanical systems obey a probabilistic behavior. As the position and momentum can never be determined at the starting point, the position (or momentum) in the future cannot be precisely predicted, only the probability of either of them. This is manifested in the postulate that all properties, present or future, of a particle are contained in a quantity known as the wavefunction Ψ of a system. This function, in general, depends on spatial coordinates and time; thus, for a one-dimensional motion (to be discussed first), the wavefunction is written as $\Psi(x, t)$. The probability of finding a quantum mechanical system is given by the

integral of the square of this wavefunction: $\int \Psi(x,t)^2\, dx$. Any property $\langle o \rangle$ one wishes to observe for the system is expressed as the "expectation value" of the operator $\hat{O}$ associated with the property, where the expectation value is defined as

$$\langle o \rangle = \frac{\int \Psi(x,t)\ \hat{O}\, \Psi(x,t) dx}{\int \Psi(x,t)\ \Psi(x,t) dx} \tag{1.38}$$

As discussed earlier, a diatomic molecule possesses only one degree of vibrational freedom, the periodic elongation and compression of the bond connecting the two atoms that will be designated the x coordinate in the following discussion. Thus, the total energy, in analogy to Eq. 1.2, of an oscillating diatomic molecule can be written as the sum of kinetic energy T and potential energy V:

$$E = T + V \tag{1.39}$$

The kinetic energy is written in terms of classical physics as

$$T = \frac{1}{2}mv^2 \quad \text{or} \quad 2T = \frac{p^2}{2m} \tag{1.40}$$

where the momentum is given by $p = mv$. Here, v is the velocity and m is the reduced mass of the oscillating diatomic molecule, defined earlier (Eq. 1.25). In quantum mechanics, the classical momentum is substituted by the momentum operator $\hat{p}$,

$$\hat{p} = \frac{\hbar}{i}\ \frac{d}{dx} \tag{1.41}$$

where $\hbar$ is Planck's constant, divided by 2π, and i is the imaginary unit, defined by $\sqrt{-1} = i$. This substitution of the classical momentum by a differential operator is often considered the central postulate of quantum mechanics because it cannot be derived, although it can be visualized from the classical wave equation. Equation 1.41 is a mathematical instruction that requires taking the spatial derivative of the wavefunction $\hat{p}$ is operating on, and multiplying the results by $\hbar/i = -i\hbar$ to obtain the equivalent of the classical momentum. Examples of the use of such an operator are given in the following sections.

1.4.2 Diatomic molecules: harmonic oscillator

The potential energy for a diatomic vibrating system is discussed next. This potential function is shown schematically in Figure 1.3, and can be obtained by detailed quantum mechanical calculations, in which the electronic energy is computed as a function of the internuclear distance. This potential energy can be approximated by the Morse potential, given by

$$V(x) = D_e\ \{1 - \ e^{-a(x-x_0)}\}^2 \tag{1.42}$$

with

$$a = \sqrt{\frac{k}{2D_e}}\ [(\mathrm{N\,m^{-1}/J})^{1/2} = \mathrm{m^{-1}}]$$

The function has a minimum at the bond equilibrium distance x_0. When compressing the bond beyond x_0, the potential energy rises sharply because of the repulsion of the two atoms. When the bond is elongated toward large interatomic distances, the potential function eventually levels out, and the bond breaks. One normally defines the potential energy at very large interatomic distances as the zero energy (no bonding interaction takes

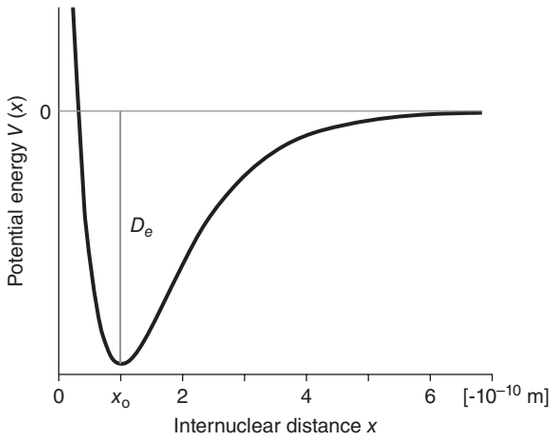

Figure 1.3 *Graph of the potential energy function for a diatomic molecule. Parameters are specified in Eq. 1.58*

place at large distances); thus, the potential energy of the bond is at a negative minimum at the equilibrium distance. The energy difference between zero potential energy and the minimum potential energy at point x_0 is referred as the bond dissociation energy, D_e.

Solving the quantum mechanical equations for the vibrations of a diatomic molecule with the potential function shown in Figure 1.3 would be difficult. Thus, one approximates the shape of the potential function in the vicinity of the potential energy minimum by a more simplistic function by expanding the potential energy $V(x)$ in a power series about the equilibrium distance:

$$V(x) = V(x_0) + (x - x_0)\left(\frac{dV}{dx}\right)_{x=x_0} + \frac{1}{2!}(x - x_0)^2\left(\frac{d^2V}{dx^2}\right)_{x=x_0} + \frac{1}{3!}(x - x_0)^3\left(\frac{d^3V}{dx^3}\right)_{x=x_0} + \cdots \quad (1.43)$$

$V(x_0)$ is an offset along the Y-axis and does not affect the curvature of the potential energy. The term containing the first derivative of the potential energy with respect to x is zero because the equilibrium geometry corresponds to an energy minimum. Terms higher than the quadratic expression in Eq. 1.43 are ignored at this point. Thus, one approximates the potential energy $V(x)$ by

$$V = (x - x_0)^2\left(\frac{d^2V}{dx^2}\right)_{x=x_0} \approx \frac{1}{2}kx^2 \quad (1.44)$$

which also could have been obtained by integrating

$$F = -kx \quad (1.23)$$

for a system obeying Hook's law.

Thus, to a first approximation, one assumes that the chemical bond in a diatomic molecule obeys Hook's law, just as the motion of two spring-coupled masses. Combining Eqs. 1.39, 1.41, and 1.43, the vibrational Schrödinger equation for a two-particle system with one degree of freedom (x) is then:

$$\left\{-\frac{\hbar^2}{2m}\frac{d^2}{dx^2} + \frac{1}{2}kx^2\right\}\psi(x) = E\psi(x) \quad (1.45)$$

This differential equation is known as "Hermite's" differential equation, in which the wavefunctions $\psi(x)$ are the time-independent (stationary-state) vibrational wavefunctions, and E denotes the vibrational eigenvalues.

Equation 1.45 is a typical operator – eigenvalue equation notation commonly used in linear algebra. This formalism is an instruction to operate with an operator, here, the *vibrational Hamiltonian* $\hat{H}_{\text{vib}}$

$$\hat{H}_{\text{vib}} = \left\{ -\frac{\hbar^2}{2m} \frac{d^2}{dx^2} + \frac{1}{2} kx^2 \right\} \tag{1.46}$$

on a set of (yet unknown) functions to obtain the eigenvalues. Substituting the eigenvalues into a trial solution and considering the boundary conditions yields the eigenfunctions $\psi(x)$. In Appendix A, a much simpler system, the so-called particle-in-a-box, is discussed in detail to show the process of obtaining the eigenvalues and eigenfunctions in a model system. Detailed procedures for solving the vibrational Schrödinger equation 1.46 can be found in most quantum chemistry textbooks, and are summarized in Appendix B. Here, only the results of the mathematical solution are presented.

The vibrational wavefunctions resulting from the discussion in Appendix B are of the form

$$\psi_n(x) = NH_n\left(\sqrt{\alpha}\, x\right) e^{-\frac{\alpha x^2}{2}} \tag{1.47}$$

where N is a normalization constant, $N = \left(\frac{\alpha}{\pi}\right)^{1/4}$ and $H_n(x)$ are the Hermite polynomials of order n in the variable x, n is an integer, the vibrational quantum number, which may take values from zero to infinite, and

$$\alpha = \frac{2\pi\nu m}{\hbar} \tag{1.48}$$

All other symbols have their usual meaning. Setting $z = \left(\sqrt{\alpha}\, x\right)$, the Hermite polynomials in the variable z are

$$\begin{aligned} H_0(z) &= 1 \\ H_1(z) &= 2z \\ H_2(z) &= 4z^2 - 2 \\ H_3(z) &= 8z^3 - 12z \end{aligned} \tag{1.49}$$

The order n of the Hermite polynomial determines the highest power in which the variable z occurs in each polynomial. Thus, more highly excited states (i.e., those with higher quantum number n) correspond to Hermite polynomials with higher power of z. This aspect is important because the power of z determines the shape of the wavefunctions.

The higher members of the Hermite polynomials can be derived from the recursion formula:

$$z\, H_n(z) = nH_{n-1}(z) + \frac{1}{2} H_{n+1}(z) \tag{1.50}$$

Thus, the Hermite polynomial of degree n is related to the previous and subsequent polynomials. The first few vibrational wavefunctions thus are:

$$\begin{aligned} \psi_0(x) &= \left(\frac{\alpha}{\pi}\right)^{1/4} e^{-\frac{\alpha x^2}{2}} \\ \psi_1(x) &= \left(\frac{\alpha}{\pi}\right)^{1/4} 2\left(\sqrt{\alpha} x\right) e^{-\frac{\alpha x^2}{2}} \\ \psi_2(x) &= \left(\frac{\alpha}{\pi}\right)^{1/4} \left(4\alpha x^2 - 2\right) e^{-\frac{\alpha x^2}{2}} \\ &\ldots \end{aligned} \tag{1.51}$$

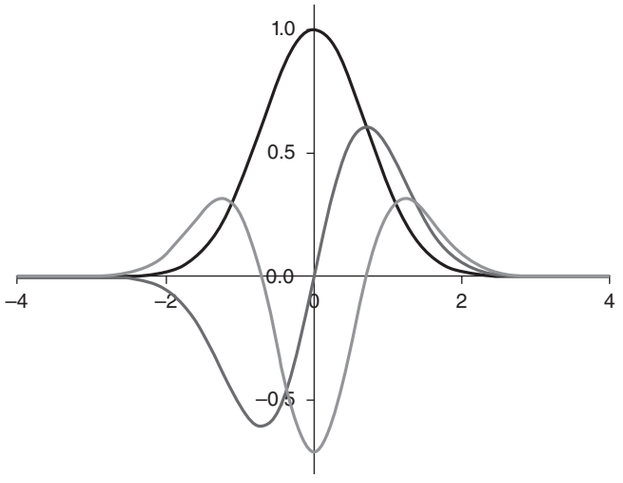

Figure 1.4 *Plot of the first three vibrational wavefunctions, which are products of a polynomial function that becomes very large with increasing* x *and a Gaussian function that decreases exponentially with* x*, resulting in the depicted curves for* n = *0 (black),* n = *1 (dark gray), and* n = *2 (light gray)*

These functions, which are shown in Figure 1.4, form an orthonormal vector space. Orthonormality implies that

$$\int_{-\infty}^{\infty} \psi_i(x)\psi_j(x)\,dx = \delta_{ij} = \begin{cases} 1 & \text{if } i = j \\ 0 & \text{if } i \neq j \end{cases} \tag{1.52}$$

Here, δ_{ij} represents the Kronecker delta, which equals to one if $i = j$ and zero otherwise.

For example,

$$\int_{-\infty}^{\infty} \psi_0(x)\psi_0(x)\,dx = \sqrt{\frac{\alpha}{\pi}} \int_{-\infty}^{\infty} e^{-\alpha x^2} dx = \sqrt{\frac{\alpha}{\pi}}\sqrt{\frac{\pi}{\alpha}} = 1 \quad \text{and}$$

$$\int_{-\infty}^{\infty} \psi_0(x)\psi_1(x)\,dx = \sqrt{\frac{\alpha}{\pi}} \int_{-\infty}^{\infty} 2\,(\sqrt{\alpha}x) e^{-2\alpha x^2} dx = 0 \tag{1.53}$$

In Eq. 1.53, the integral relationship $\int_{-\infty}^{\infty} e^{-\alpha x^2} dx = \sqrt{\frac{\pi}{\alpha}}$ was used.

The orthogonality of the vibrational wavefunctions can also be demonstrated by graphical integration, as demonstrated in Section 1.5.

The eigenvalues of the vibrational Schrödinger equation (Eq. 1.46) are given by

$$E_n = \left(n + \frac{1}{2}\right) h\nu \tag{1.54}$$

In Eq. 1.54, the frequency ν is written in units of s^{-1} such that the term $h\nu$ has units of energy (J). Vibrational spectroscopists, however, prefer to use wavenumber as a unit of energy; thus, in the remainder of the book the vibrational energy is expressed as

$$E_n = \left(n + \frac{1}{2}\right) hc\tilde{\nu} \tag{1.55}$$

and the expressions $h\nu$, $hc\tilde{\nu}$, and $\hbar\omega$ are used to denote the energy of photons, where ω is the angular frequency, defined by

$$\omega = 2\pi\nu \tag{1.56}$$

The harmonic oscillator wavefunctions and energy eigenvalues are shown in Figure 1.5, along with the quadratic potential energy function used to define the vibrational Schrödinger equation, and the energy levels corresponding to Eq. 1.54. There are several interesting facets about the wavefunctions and energy level plot. First of all, Eq. 1.54 and Figure 1.5 demonstrate that even in the vibrational ground state with $n = 0$, the system is not at zero energy, but rather, at energy

$$E_0 = \frac{1}{2} h\nu \tag{1.57}$$

which is referred to as the zero-point energy. This zero-point energy accounts for the fact that even in its vibrational ground state, the atoms in a molecule undergo continuous vibrational motion along the normal modes derived earlier. Photons may cause a transition into more highly excited states of these vibrational coordinates. This zero-point vibrational energy also accounts for the third law of thermodynamics, which states that absolute zero temperature is unattainable. This is because atomic "stand-still" is impossible because of the residual vibrational energy. This is also in line with Heisenberg's uncertainty principle (Eq. 1.37), because a vibrational amplitude of zero would define both position and momentum simultaneously. Figure 1.5 also indicates some degree of "tunneling," or a finite probability of the oscillating system to be found outside the potential energy curve. Furthermore, the wavefunctions are symmetric ($n = 0, 2, 4, \ldots$) or antisymmetric ($n = 1, 3, 5, \ldots$) with respect to the X_0 line. This aspect will become particularly important in the discussion of the allowed and forbidden transitions in the harmonic oscillator approximation. Finally, the quadratic potential depicted in Figure 1.5 would not explain bond breakage at sufficiently high energy, because the potential function – the restoring force between the oscillating energy increases steadily in the "harmonic approximation." Therefore, the concept of an anharmonic potential needs to be introduced.

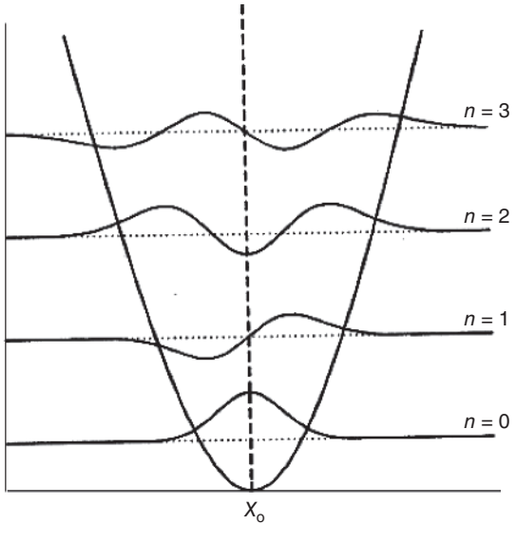

Figure 1.5 *Quadratic potential energy function* $V = 1/2kx^2$ *for a diatomic molecule and the resulting quantum mechanical vibrational wavefunctions*

1.4.3 Diatomic molecules: anharmonicity

The potential energy function used so far, $V = \frac{1}{2}k\,x^2$ (Eq. 1.44), is a gross approximation of the real potential energy function shown in Figure 1.3, and therefore, needs to be modified. The next level of approximation involves the inclusion of higher terms in the original expression (Eq. 1.43) for the potential energy:

$$V(x) = \frac{1}{2!}\,(x - x_0)^2 \left(\frac{d^2V}{dx^2}\right)_{x=x_0} + \frac{1}{3!}\,(x - x_0)^3 \left(\frac{d^3V}{dx^3}\right)_{x=x_0} \tag{1.58}$$

Using the same simplification of the series expansion of the potential energy and setting the cubic force constant

$$k' = \left(\frac{d^3V}{dx^3}\right)_{x=x_0} \tag{1.59}$$

one can write the anharmonic vibrational Schrödinger equation as

$$\left\{ -\frac{\hbar^2}{2m}\,\frac{d^2}{dx^2} + \frac{1}{2}\,kx^2 + \frac{1}{6}\,k'x^3 \right\} \psi(x) = E\psi(x) \tag{1.60}$$

Equation 1.60 is solved by perturbation methods and yields the perturbed energy eigenvalues for a diatomic molecule

$$E_n = \left(n + \frac{1}{2}\right) h\nu \; - \; \left(n + \; \frac{1}{2}\right)^2 h\nu\chi = \left(n + \; \frac{1}{2}\right) h\nu \; - \frac{\left(n + \frac{1}{2}\right)^2 h^2\nu^2}{4D_e} \tag{1.61}$$

with

$$\chi = \frac{h\nu}{4D_e} \tag{1.62}$$

As χ always is a positive number, the energy levels of the anharmonic case are always lowered as compared to the harmonic oscillator; this lowering increases with the square of the quantum number *n.* This is depicted in Figure 1.6, which shows a comparison between harmonic and anharmonic oscillator energy levels.

In addition to lowering the energy values, the wavefunctions will be shifted toward longer internuclear distances; consequently, the symmetry of the wavefunctions changes and they are no longer symmetric or antisymmetric with respect to the x_0 position. This fact changes the selection rules that determine which transitions are allowed for diatomic molecules.

At this point, some calculations and examples are presented in order to transmit a feeling for magnitudes involved. For a common chemical moiety, the bond energy is typically around $1000\,\mathrm{kJ\,mol^{-1}}$. Expressing this quantity in molecular, rather than molar units (dividing by Avogadro's number), one finds that the bond dissociation energy D_e used in Eq. 1.42 is

$$D_e = 1.5 \times 10^{-18}\ \mathrm{J/molecule} = 75,000\ \mathrm{cm^{-1}} \tag{1.63}$$

In Eq. 1.63, the energy conversion $E = hc\tilde{\nu}$ or $1\ \mathrm{J} = 6.6 \times 10^{-34} \times 3 \times 10^{10} \approx 2 \times 10^{-23}\ \mathrm{cm^{-1}}$ was used with the velocity of light c expressed in $\mathrm{cm\,s^{-1}}$. Vibrational force constants, as defined in Eq. 1.31, are found to be around $500\,\mathrm{N\,m^{-1}}$ for a typical chemical bond. Equation 1.42 was used with

$$a = 1 \times 10^{10}\ \mathrm{m^{-1}} \quad \text{and} \quad x_0 = 100\ \mathrm{pm} = 10^{-10}\ \mathrm{m}$$

to calculate the potential energy curve shown in Figure 1.3. As pointed out earlier, a typical vibrational energy for a diatomic molecules with a force constant of $500\,\mathrm{N\,m^{-1}}$ is about $3000\,\mathrm{cm^{-1}}$; thus, one finds that the spacing between (harmonic) vibrational energy levels is only about 1/25th of the depth of the potential well for a strong bond. Thus, many vibrational quanta of light are necessary to raise the energy of a bond

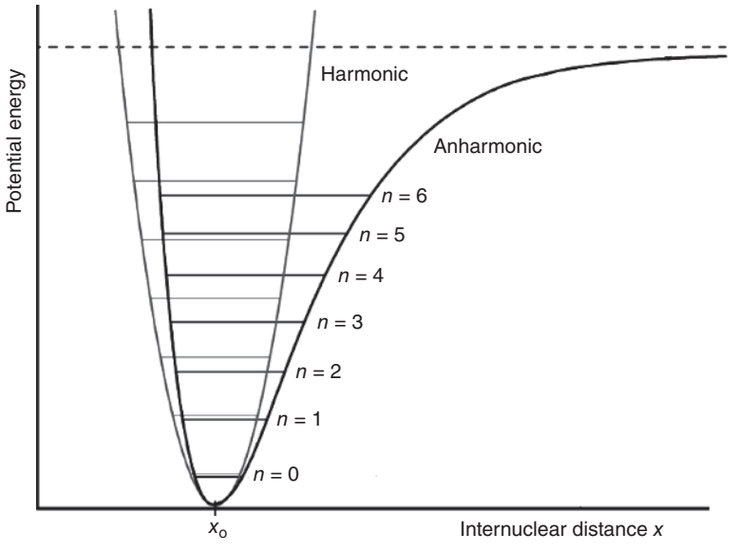

Figure 1.6 *Comparison of energy levels for harmonic and anharmonic oscillators*

stretching vibration such that bond dissociation occurs. However, bond breakage virtually never happens through consecutive absorption of IR photons because of several factors, among them are the short lifetime of vibrational states and the fast (nonradiative) dissipation of the vibrational energy into other vibrational modes. In addition, because the spacing between vibrational levels gets smaller for real molecular systems owing to the anharmonicity of the potential function, photons of different energy would be needed to raise the energy to the higher levels through consecutive absorption processes. On the other hand, the process of raising the vibrational energy from the ground state directly to an excited state near the dissociation limit is low because of the small transition moment. Thus, one concludes that bond breakage occurs mostly through mechanisms different from direct vibrational excitation.

In summary, diatomic molecules were described in both the harmonic and anharmonic approximations. The vibrational wavefunctions defined in Eq. 1.51, and depicted in Figure 1.5, represent the time-independent or stationary-state vibrational wavefunctions for a diatomic molecule. The stationary-state wavefunctions of the particle-in-a-box, discussed in Appendix A, have similar appearance and symmetries, albeit completely different equations. The symmetry of wavefunctions plays an important role determining whether transitions from one to another state are allowed or forbidden. It was pointed out earlier that the unperturbed harmonic oscillator wavefunctions are symmetric with respect to X_0 (*cf.* Figure 1.5) for even quantum numbers n and antisymmetric for odd numbers of n. Therefore, one often refers to "even" and "odd" parity when describing these wavefunctions, and it is easy to see that the particle-in-a-box wavefunctions follow a similar even/odd pattern as do the harmonic oscillator wavefunctions. Furthermore, as the symmetry of the wavefunctions is distorted in the anharmonic approximation, the selection rules will change drastically.

1.4.4 Polyatomic molecules

Section 1.3 demonstrated how the treatment of diatomic molecules could be extended toward polyatomic molecules, and introduced the concepts of normal modes of vibration and normal coordinates for the classical description of the vibrations of polyatomic molecules. In complete analogy, the quantum mechanical treatment can be extended from the case of diatomic molecules toward polyatomic molecules.

For a diatomic molecule, the vibrational Schrödinger equation was found to be

$$\left\{ -\frac{\hbar^2}{2m}\frac{d^2}{dx^2} + \frac{1}{2}kx^2 \right\} \psi(x) = E\psi(x) \tag{1.45}$$

In analogy, the vibrational Schrödinger equation for a polyatomic molecule, written in terms of the normal coordinates (*cf.* Eq. 1.34), is

$$-\frac{\hbar^2}{2}\frac{d^2\psi_{\text{vib}}}{dQ^2} + \frac{1}{2}\Lambda Q^2\psi_{\text{vib}} = E_{\text{vib}}\psi_{\text{vib}} \tag{1.64}$$

where ψ_{vib} is the total vibrational wavefunction of the molecule. Next, one writes ψ_{vib} as a product of the wavefunctions along each of the $3N-6$ normal coordinates:

$$\psi_{\text{vib}} = \psi_1(Q_1) \cdot \psi_2(Q_2) \cdot \psi_3(Q_3) \cdot \cdots \tag{1.65}$$

This definition of the total vibrational wavefunction as products of wavefunctions associated with one and only one normal coordinate succeeds because the expressions for kinetic and potential energies are both diagonal in normal coordinate space (*cf.* Eqs. 1.33 and 1.34). Substitution of Eq. 1.65 into Eq. 1.64 yields the Schrödinger equation in terms of the $3N-6$ normal coordinates:

$$-\frac{\hbar^2}{2}\sum_{k=1}^{3N-6}\frac{d^2\psi_k}{dQ_k^2} + \frac{1}{2}\sum_{k=1}^{3N-6}\Lambda_k Q_k^2\psi_k = E_{\text{vib}}\psi_k \tag{1.66}$$

As the normal coordinates Q_k are orthogonal functions, and because – in normal coordinate space – the kinetic and potential energies are in diagonal form (see Eqs. 1.33 and 1.34), Eq. 1.66 can be separated into $3N-6$ individual differential equations of the form

$$-\frac{\hbar^2}{2}\frac{d^2\psi_k}{dQ_k^2} + \frac{1}{2}\Lambda_k Q_k^2\psi_k = E_k\psi_k \tag{1.67}$$

with the energy eigenvalues (in wavenumber units) given by

$$E_k(n) = \left(n_k + \frac{1}{2}\right) hc\tilde{\nu}_k \tag{1.68}$$

and

$$E_{\text{vib}} = \sum_{k=1}^{3N-6} E_k \tag{1.69}$$

In analogy with the diatomic molecules, one writes the solutions of Eq. 1.67 as the eigenfunctions

$$\psi_n(Q_k) = NH_n(\sqrt{\alpha}\,Q_k)\, e^{-\frac{\alpha Q_k^2}{2}} \tag{1.70}$$

The results of this quantum mechanical discussion are shown in Figure 1.7 for a triatomic molecule, such as water. Here, the vibrational frequencies associated with each normal coordinate are approximately given by

$$\tilde{\nu}_1(Q_1) = 3750\ \text{cm}^{-1} \quad \tilde{\nu}_2(Q_2) = 3650\ \text{cm}^{-1} \quad \tilde{\nu}_3(Q_3) = 1620\ \text{cm}^{-1}$$

The energy level diagram, in the harmonic approximation, consists of three energy ladders (see Figure 1.7), one for each normal coordinate. Note that each ladder starts at

$$E_k(0) = \left(\frac{1}{2}\right) hc\tilde{\nu}_k \tag{1.71}$$

that is, at approximately 1875, 1825, and 810 cm^{-1} for Q_1, Q_2, and Q_3, respectively.

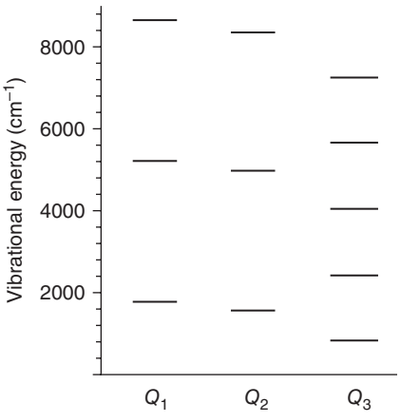

Figure 1.7 *Energy ladder diagram for a triatomic molecule within the harmonic oscillator approximation*

Thus, the total zero-point vibrational energy of water is given by $E_0^T = E_0(Q_1) + E_0(Q_2) + E_0(Q_3) = 1875 + 1825 + 810$ or approximately $4510\,\mathrm{cm}^{-1}$. In any of the energy ladders, a transition to the more highly excited vibrational state may occur if a photon of proper wavenumber (3750, 1650, or $1620\,\mathrm{cm}^{-1}$) interacts with the sample and certain requirements are fulfilled. Whether or not a transition occurs does not solely depend on the presence of photons with the correct energy, but also on some symmetry considerations. In the following section, the basic formalism is introduced that describe the interaction of light with molecular systems in their stationary energy states. This interaction is based on time-dependent processes and requires the use of time-dependent wavefunctions and the time-dependent Hamiltonian.

1.5 Time-dependent description and the transition moment

1.5.1 Time-dependent perturbation of stationary states by electromagnetic radiation

Time-independent quantum mechanics introduced in the previous sections describes the energy expressions and wavefunctions of stationary states, that is, states that do not change with time. Stationary-state wavefunctions and energies were obtained by solving the appropriate Schrödinger equations for the given system. Next, a description is needed that describes how a system can transition from one stationary state to another when a perturbation, typically electromagnetic radiation, is applied. For this, one needs to invoke the time-dependent Schrödinger equation, which for the one-dimensional case is

$$i\hbar \frac{\partial \mathbf{\Psi}(x,t)}{t} = \mathbf{H}\mathbf{\Psi}(x,t) \tag{1.72}$$

Equation 1.72 is solved by perturbation methods in which a perturbation operator H' is introduced

$$\mathbf{H} = H + H' \tag{1.73}$$

One assumes that there exist exact eigenfunctions for the operator H, and that the perturbation due to H' is small. If the perturbation applied to the system is due to electromagnetic radiation, one may write the perturbation operator as

$$H'(t) = -\mathbf{E}_x^0 \sum\nolimits_i e_i x_i \left\{ \cos\left(2\pi\nu t + \frac{2\pi z}{\lambda}\right)\right\} \tag{1.74}$$

In Eq. 1.74, electromagnetic radiation propagating in the z-direction is assumed, with the electric vector along the x-direction. The electric field

$$\mathbf{E}_x = \mathbf{E}_x^0 \left\{ \cos\left(2\pi\nu t + \frac{2\pi z}{\lambda}\right)\right\} \tag{1.75}$$

will exert a force

$$\mathbf{F} = e\mathbf{E} \tag{1.76}$$

on particles with charge e. If the molecular system consists of i charged particles found at positions x_i, one defines the "electric dipole operator" $\boldsymbol{\mu}$ according to

$$\boldsymbol{\mu} = \sum\nolimits_i e_i x_i \tag{1.77}$$

and rewrites Eq. 1.75 as

$$H'(t) = -\mathbf{E}_x^0\, \boldsymbol{\mu} \left\{ \cos\left(2\pi\nu t + \frac{2\pi z}{\lambda}\right)\right\} \tag{1.78}$$

The time-dependent Schrödinger equation

$$i\hbar \frac{\partial \boldsymbol{\Psi}(x,t)}{\partial t} = \left[H - \mathbf{E}_x^0 \boldsymbol{\mu} \left\{ \cos\left(2\pi\nu t + \frac{2\pi z}{\lambda}\right)\right\}\right] \boldsymbol{\Psi}(x,t) \tag{1.79}$$

subsequently is solved with the unperturbed eigenfunctions ψ of the H operator

$$H\psi(x) = E\psi(x) \tag{1.80}$$

which may be, for example, the time-independent (unperturbed) wavefunctions of the harmonic oscillator. The time dependence of each of the wavefunctions $\psi(x)$ is introduced as follows:

$$\Psi(x,t) = \varphi(t)\psi(x) \tag{1.81}$$

where

$$\varphi(t) = e^{i\omega t} \tag{1.82}$$

Equation 1.81 is the general definition of a time-dependent wavefunction that consists of a stationary, time-independent part, $\psi(x)$ and the time evolution of this wavefunction, given by $\varphi(t) = e^{i\omega t}$.

The time-dependent wavefunctions $\boldsymbol{\Psi}(x,t)$ of the system undergoing a transition subsequently are expressed in terms of time-dependent coefficients $c_k(t)$ and the time-dependent wavefunctions $\boldsymbol{\Psi}(x,t)$ according to

$$\boldsymbol{\Psi}(x,t) = \sum\nolimits_k c_k(t)\Psi(x,t) = \sum\nolimits_k c_k(t)\varphi(t)\psi(x) \tag{1.83}$$

The coefficients $c_k(t)$ describe the time-dependent response of the quantum mechanical system to the perturbation; in particular, the change in population of the excited state in response to the perturbation. An example may serve to illustrate the procedure invoked so far. Consider a two-state system in the absence of a perturbation, where the splitting between the ground-state energy level $\psi_g(x)$ and the excited-state energy level $\psi_e(x)$ is much larger than thermal energy (see Eqs. 1.101–1.103).

Thus, the system is in the ground state, and can be described by $c_g(t) = 1$ and $c_e(t) = 0$ or

$$\boldsymbol{\Psi}(x,t) = 1\ \varphi_g(t)\ \psi_g(x) + 0\ \varphi_e(t)\ \psi_e(x) \tag{1.84}$$

After a perturbation is applied, the coefficients $c_g(t)$ and $c_e(t)$ change to account for the system undergoing a transition into the excited state that can be described by

$$\boldsymbol{\Psi}(x,t) = 0\ \varphi_g(t)\ \psi_g(x) + 1\ \varphi_e(t)\ \psi_e(x) \tag{1.85}$$

Thus, the overall time-dependent Schrödinger equation that accounts for the response of the system is

$$i\hbar\frac{\partial\left[\sum_k c_k(t)\ \varphi(t)\psi(x)\right]}{\partial t} = \left[H - \mathbf{E}_x^0\boldsymbol{\mu}\ \left\{\cos\left(2\pi\nu t + \frac{2\pi z}{\lambda}\right)\right\}\right]\left[\sum_k c_k(t)\,\varphi(t)\ \psi(x)\right] \tag{1.86}$$

The solution of this equation can be found in many texts on quantum mechanics (*cf*. Ref. [3, vol. II, Chapter 2]), and it proceeds by taking the necessary derivatives and integrating the resulting terms $\frac{dc_k}{dt}$ between time 0 and the duration of the perturbation. This procedure yields an expression for the time evolution of the expansion coefficients $c_m(t)$:

$$c_m(t) = \delta_{nm} + \frac{iE^0}{2\hbar}\langle\psi_n|\ \mu|\psi_m\rangle\ \left[\frac{e^{i(\omega_{nm}+\omega)t}-1}{(\omega_{nm}+\omega)} + \frac{e^{i(\omega_{nm}-\omega)t}-1}{(\omega_{nm}-\omega)}\right] \tag{1.87}$$

Equation 1.87 is one of the most important equations for understanding spectroscopic processes because it outlines three major features of the response of a molecule when exposed to electromagnetic radiation. First, it implies that the term $\langle\psi_n|\mu|\psi_m\rangle$, known as the transition moment, must be nonzero. The transition moment describes the action of the dipole operator μ defined in Eq. 1.77 on the stationary-state wavefunctions ψ_n and ψ_n between which the transition is induced. The transition moment, in general, determines the selection rules, depending on the exact nature of the wavefunctions and their symmetries. This aspect is discussed in the following section. Second, the term containing the amplitude of the electric field, E^0, indicates that the "light must be on" for a transition to occur. Third, the part in the square brackets in Eq. 1.87 describes how the system responds to electromagnetic radiation of different frequency or wavelength. Thus, it is this term that prescribes that the frequency of the light must match the energy difference between the molecular energy levels. This can be seen from the following discussion. The second term in the square bracket becomes very large at the resonance condition,

$$\omega_{nm} = \omega \tag{1.88}$$

which implies that when the frequency ω of the incident radiation is equal to, or very close to, the energy difference ω_{nm} between states n and m, a transition between these states may occur and a photon with the corresponding energy $\hbar\omega$ may be absorbed, if the transition moment is nonzero.

Similarly, the first term in the square bracket in Eq. 1.87 becomes very large if

$$\omega_{nm} = -\omega \tag{1.89}$$

This case corresponds to the situation of stimulated emission, where a photon of the proper energy impinges onto a molecular or atomic system in the excited state and causes this state to emit a photon, thereby returning to the lower energy state. This time-dependent part of Eq. 1.87 also contains explicitly the expressions needed to explain certain off-resonance phenomena, such as molecular polarizability, to be discussed in Section 1.6 and Chapter 4. The magnitude of resonance *vs.* off-resonance effects can be estimated from the expression in square brackets as well.

Equation 1.87 holds for one-photon absorption and emission situations that include standard IR (vibrational), microwave (rotational), and visible/ultraviolet (electronic) absorption spectroscopies. The time-dependent part in the square bracket of Eq. 1.87 can be summarized as

$$\Delta E_{\text{molecule}} = (h\nu)_{\text{photon}} \tag{1.90}$$

This equation was first mentioned in the introduction, and it corresponds exactly to the condition as described in Eqs. 1.88 and 1.89:

$$(\omega_{nm} = \pm\,\omega) \tag{1.91}$$

1.5.2 The vibrational transition moment for absorption: harmonic diatomic molecules

The previous section demonstrated that three conditions are necessary for a transition to occur in an atomic or a molecular system under the influence of a perturbation by electromagnetic radiation. First, radiation must impinge on the molecular system ($E^0 \neq 0$); second, the radiation must possess the proper energy, or frequency, corresponding to the energy difference between the molecular or atomic states. This part is fulfilled by the conditions listed in Eqs. 1.88–1.91. The third condition that must be fulfilled is that the dipole transition moment must be nonzero:

$$\langle \boldsymbol{\mu} \rangle_{nm} = \int \psi_n \mu \psi_m d\tau = \langle \psi_n | \mu | \psi_m \rangle \tag{1.92}$$

In Eq. 1.92, the integration extends over all space, as indicated by the differential $d\tau$. Here, as pointed out earlier, ψ_n and ψ_m are the stationary-state wavefunctions associated with energy levels n and m. For IR absorption spectroscopy, these wavefunctions are the vibrational wavefunctions defined in Eq. 1.51; furthermore, as given in Eqs. 1.102–1.104, the lower energy state and wavefunction normally correspond to the ground state, ψ_0. Thus, one may rewrite Eq. 1.92 as

$$\langle \boldsymbol{\mu} \rangle_{e0} = \langle \psi_e | \mu \, | \psi_0 \rangle \neq 0 \tag{1.93}$$

where ψ_e represents a vibrationally excited state. For a transition to occur, the transition moment $\langle \boldsymbol{\mu} \rangle_{e0}$ must be nonzero. Whether the transition moment for a vibrational transition is zero or not depends on the geometry of the molecule and on the polarity of the atoms, which will be discussed later in detail. However, it is instructive even at this early point in this text to point out that certain vibrational modes have a zero transition moment and cannot be observed in the IR absorption spectrum. A typical example for this is the symmetric stretching mode of CO_2, where both oxygen atoms move away from the central C atom in phase and with equal amplitudes (see Chapter 2). Although the energy of this vibrational mode is well known (from the Raman spectrum), irradiation of CO_2 molecules with IR radiation of this energy does not produce a transition, because the transition moment is zero for symmetry reasons.

Next, the transition moment

$$\langle \boldsymbol{\mu} \rangle_{e0} = \langle \psi_e | \mu | \psi_0 \rangle \neq 0 \tag{1.93}$$

for harmonic oscillator wavefunctions is presented, with particular emphasis of the transition between the ground and first excited states, for which Eq. 1.93 can be written as

$$\begin{aligned} \langle \boldsymbol{\mu} \rangle_{10} = & \langle \psi_1 | \mu | \psi_0 \rangle = \int_{-\infty}^{\infty} \psi_1(x) \mu \psi_0(x) \, dx \\ = & e \int_{-\infty}^{\infty} \psi_1(x) \, x \psi_0(x) \, dx \end{aligned} \tag{1.94}$$

because the dipole operator for a single charged particle is just $\mu = ex$.

First, the orthogonality of the vibrational wavefunctions is demonstrated graphically in Figure 1.8(a) and (b), which demonstrates by graphical integration that the integrals $\int_{-\infty}^{\infty} \psi_1(x)\psi_0(x) \, dx$ and $\int_{-\infty}^{\infty} \psi_2(x)\psi_1(x) \, dx$ are, indeed, zero and that the vibrational wavefunctions are orthogonal. Next, it will be shown by graphical integration that the transition moment between the ground and first excited states is nonzero. When evaluating the transition moment defined by Eq. 1.94, the two wavefunctions are multiplied by the transition operator, shown by the straight line in Figure 1.8(c). This makes the product function $\psi_1(x) \, \mu\psi_0(x)$ positive for both positive and negative values of x; thus, integration along the x-axis yields a nonzero value. This result could also have been obtained by analytical integration. At this point, it is also advantageous to introduce the concept of parity. The wavefunctions shown in Figure 1.5 were previously referred to as "symmetric" or "antisymmetric" with respect to the dashed line corresponding to the equilibrium position of the harmonic oscillator.

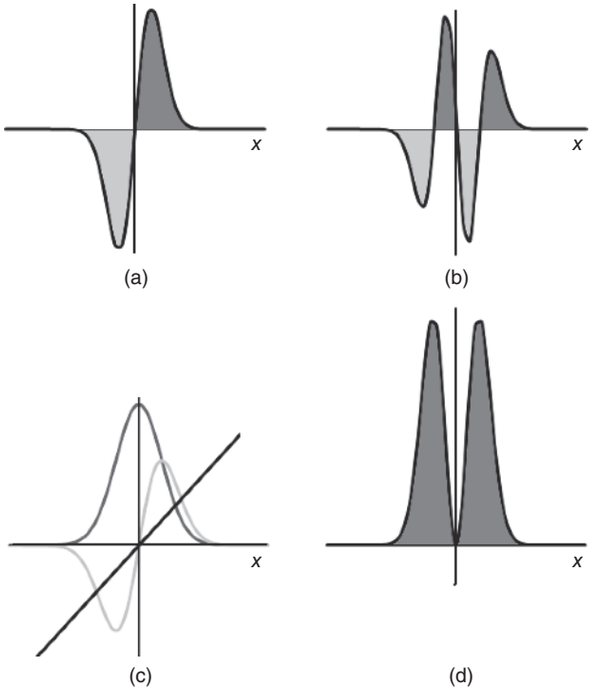

Figure 1.8 *Graphical representation of the orthogonality of vibrational wavefunctions and the vibrational transition moment. (a) Product of $\psi_0 \cdot \psi_1$. The light and dark gray regions under the curves have equal areas; thus, integration along* x *results in zero net area, and the functions are orthogonal. (b) Product of $\psi_1 \cdot \psi_2$. The same argument demonstrates that the functions are orthogonal. (c) Plot of ψ_0 (gray), ψ_1 (light gray), and the dipole operator $\mu = \mathrm{ex}$ (black). (d) Integration of $\langle \psi_1 | \mu | \psi_0 \rangle$ along* x*-axis yields a nonzero transition moment*

Similar, one can argue that the wavefunctions with quantum numbers $n = 0, 2, 4, \ldots$ have "even" parity, that is, $f(x) = f(-x)$, whereas the wavefunctions with $n = 1, 3, 5, \ldots$ have "odd" parity with $f(x) = -f(-x)$. The multiplication table for parity is

$$\begin{aligned} \text{even} \times \text{even} &= \text{odd} \times \text{odd} = \text{even} \\ \text{even} \times \text{odd} &= \text{odd} \times \text{even} = \text{odd} \end{aligned} \tag{1.95}$$

These relationships can be useful to intuitively evaluate whether or not transition moments are zero. Figure 1.8(c) and (d) demonstrates that the product of two odd functions and one even function produces an even function, as indicated by the fact that the shaded areas in (d) both are above the x-axis.

Next, the proper mathematical derivation of the selection rule for a one-photon emission or absorption for the harmonic oscillator will be presented. This derivation establishes that

$$\int_{-\infty}^{\infty} \psi_n(x) \mu \, \psi_m(x) \, dx \neq 0 \quad \text{if} \quad n = m \pm 1 \tag{1.96}$$

This proof proceeds as follows. As established earlier, the vibrational wavefunctions are of the form

$$\psi_n(x) = \left(\frac{\alpha}{\pi}\right)^{\frac{1}{4}} H_n(\sqrt{\alpha}\, x)\, e^{-\frac{\alpha x^2}{2}} \tag{1.47}$$

The Gaussian function $e^{-\frac{\alpha x^2}{2}}$ has even parity; thus, it does not affect the integral described by Eq. 1.96, and the following discussion can concentrate on the parity of the Hermite polynomials alone. Thus, the transition moment given in Eq. 1.96 can be simplified to

$$\langle \boldsymbol{\mu} \rangle_{nm} = \int H_n(x)\, x\, H_m(x)\, dx \tag{1.97}$$

where the factor $\sqrt{\alpha}$ was set to 1. Recalling the recursion formula for the Hermite polynomials,

$$xH_m(x) = mH_{m-1}(x) + \frac{1}{2}H_{m+1}(x) \tag{1.50}$$

the term $xH_m(x)$ in Eq. 1.97 can be substituted by the right-hand side of Eq. 1.50 to yield

$$\langle \boldsymbol{\mu} \rangle_{nm} = \int H_n(x) \left[mH_{m-1}(x) + \frac{1}{2}H_{m+1}(x) \right] dx \tag{1.98}$$

$$= m \int H_n(x) H_{m-1}(x) dx \; + \; \frac{1}{2} \int H_n(x)\, H_{m+1}(x)\, dx \tag{1.99}$$

As the vibrational wavefunctions, as well as the Hermite polynomials, are orthogonal (see Eq. 1.52 and Figure 1.8(a) and (b)), the two integrals in Eq. 1.99 are nonzero if and only if

$$\int H_n(x)\, H_{m-1}(x) dx = \delta_{n,m-1} \; = \begin{cases} 1 & \text{if } n = m-1 \\ 0 & \text{if } i \neq m-1 \end{cases}$$

$$\int H_n(x) H_{m+1}(x)\, dx \; = \delta_{n,m+1} = \begin{cases} 1 & \text{if } n = m+1 \\ 0 & \text{if } i \neq m+1 \end{cases} \tag{1.100}$$

Equation 1.100 implies that transitions are allowed only if the vibrational quantum number n changes by one unit, that is,

$$\Delta n = \pm 1 \tag{1.101}$$

This selection rule implies that only transitions between adjacent energy levels are allowed for the harmonic oscillator. This is shown schematically in Figure 1.9, where solid arrows indicate allowed transitions and dashed arrows indicate forbidden transitions.

1.5.3 The vibrational transition moment for absorption: anharmonic diatomic molecules

Inspection of Figure 1.6 suggests that different selection rules may hold for anharmonic diatomic molecules, because the symmetry of the wavefunctions is distorted and they cannot be classified in terms of odd/even functions with respect to the equilibrium position (or the energy minimum). Consequently, transitions that are forbidden in the harmonic oscillator, for example, transitions with $\Delta n = \pm 2, \pm 3, \ldots$ become weakly allowed for the anharmonic oscillator. Furthermore, as the energy levels are no longer equally spaced by $h\nu$ or $hc\tilde{\nu}$, the transition from $n = 1$ to $n = 2$ will have a lower energy (lower wavenumber) than the transition from $n = 0$ to $n = 1$. Thus, the vibrational spectrum of an anharmonic diatomic molecule is characterized by the presence of higher harmonics; that is, the transitions with $\Delta n = \pm 2, \pm 3$. This is shown in Figure 1.10 for gaseous bromine, Br_2. This homonuclear diatomic molecule is nonpolar; therefore, it does not exhibit an IR absorption spectrum; consequently, Figure 1.10 depicts the gas phase Raman spectra. The principles of vibrational energies of higher harmonics hold equally for IR and Raman spectra; however, the selection rules are different, which will be discussed later.

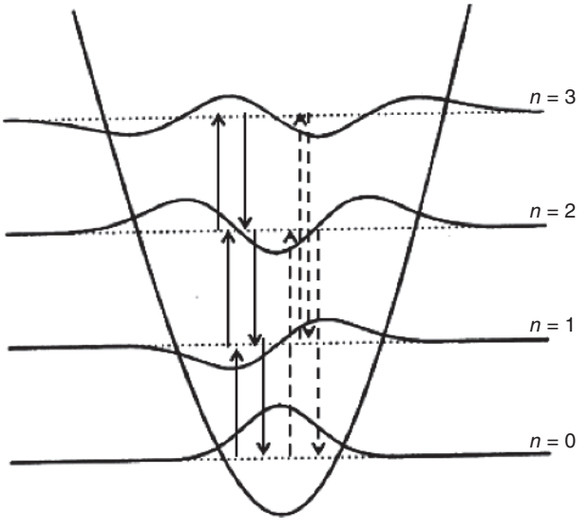

Figure 1.9 *Schematic of allowed (solid arrows) and forbidden (dashed arrows) transitions for the harmonic oscillator*

The spectra shown in Figure 1.10 further demonstrate a number of important features of vibrational spectroscopy. The inset shows an expanded region of the fundamental transition that is split into several peaks. These are, in part, due to the fact that Br_2 is a mixture of isotopic species (isotopic effects are discussed in the following section): $^{79}Br_2$, ^{79}Br–^{81}Br, and $^{81}Br_2$ with an abundance ratio of 1:2:1. Thus, the fundamental transitions exhibit these peaks at 322, 320, and 318 cm^{-1} (features f, e, and d in the inset of Figure 1.10). Furthermore, the spectrum will contain "hot bands," namely the transitions arising from states higher than the vibrational ground state. The name "hot bands" refers to the fact that these transitions are observed predominantly at elevated temperatures, to be discussed next.

So far in the discussion, it was assumed that the molecular systems are in their vibrational ground state at room temperature. This assumption is based on the Boltzmann distribution, which can be stated as

$$\frac{n_2}{n_1} = \frac{g_2}{g_1} e^{-\frac{\Delta E_{21}}{kT}} \tag{1.102}$$

In Eq. 1.102, n_2 and n_1 refer to the populations of a higher and a lower energy states, respectively, and g_2 and g_1 to their degeneracy (see Chapter 2). ΔE_{21} refers to the energy difference between the states, with $E_2 > E_1$, T is the absolute temperature, and k is Boltzmann's constant, defined as the gas constant R divided by Avogadro's number, N:

$$k = \frac{R}{N} \tag{1.103}$$

k has the value of 1.38×10^{-23} J K^{-1} or 0.695 cm^{-1} K^{-1}. The effect of the Boltzmann distribution on the population of ground and first vibrational states is best illustrated by two examples. For HCl, the vibrational transition between the ground and first excited states occurs at about 2990 cm^{-1}; that is, ΔE_{21} in Eq. 1.102 is 2990 cm^{-1}. Thus, the ratio of first excited to ground state populations is given at room temperature (298 K) by

$$\frac{n_2}{n_1} = e^{\frac{-2990}{0.695 \cdot 298}} = e^{-14.44} \approx 5.4 \times 10^{-7} \tag{1.104}$$

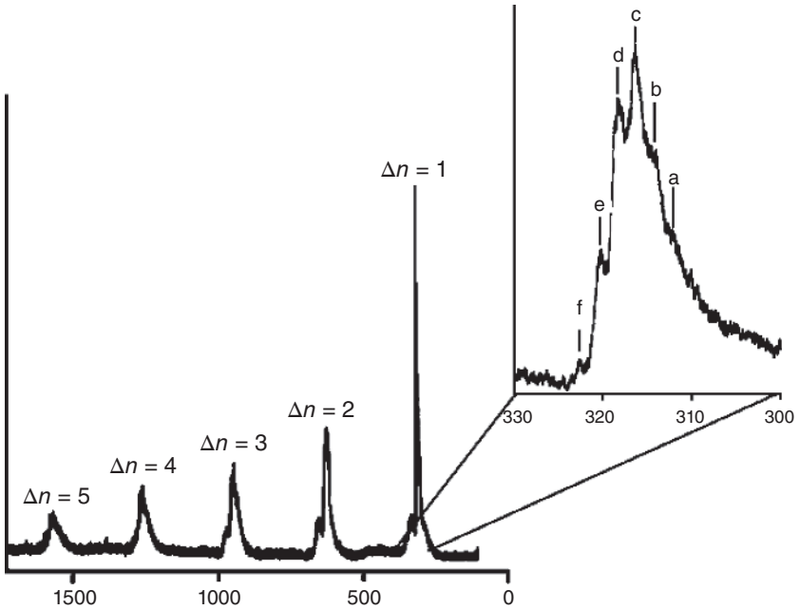

Figure 1.10 *Gas phase Raman spectrum of Br_2 with overtones and hot bands. See text for details. Baierl and Kiefer, 1975, [4]. Reproduced with permission from AIP*

Thus, for HCl at room temperature, one finds that the population of the ground state exceeds that of the excited state by a factor of more than 1 million to 1. The situation is markedly different for a heavy diatomic molecule, such as Br_2, for which the vibrational stretching frequency is much lower, namely 320 cm^{-1}:

$$\frac{n_2}{n_1} = e^{\frac{-320}{0.695 \cdot 298}} = e^{-1.545} \approx 0.21 \tag{1.105}$$

Here, the ratio of populations between the first excited and ground states is on the order of 20%. Raising the temperature of a sample, of course, has a similar effect than lowering the vibrational energy difference between states because the exponent gets smaller, and the ratio of population gets larger. This explains the "hot band" designation of the low-frequency shoulder of the stretching fundamental absorption as the temperature is raised. As indicated earlier, the frequency of the "hot band" is lower than that of the fundamental because the spacing between the $n=1$ and $n=2$ states is smaller than that of the $n=0$ and $n=1$ states. Some of the hot bands observed in the vibrational spectrum of Br_2 are shown in Figure 1.10 as well. These features are marked a, b, and c in the inset. As expected, their transition wavenumbers are lower than those of the $n=0$ to $n=1$ transition; their intensities here are exaggerated by the fact that several hot bands of several isotopomers occur at the same wavenumber [4].

In principle, one could also observe transitions from the $n=1$ to $n=2$ state from species that were not excited thermally (by collisional energy transfer) but rather by prior absorption of a photon that promoted the system into the excited state. Such cases are, however, extremely rare, because the lifetime of vibrational states, in general, is quite short (on the order of 10^{-12}–10^{-14} s); thus, to induce successive transitions, a very high photon flux is required.

1.5.4 The vibrational transition moment for absorption: polyatomic molecules

Within the harmonic oscillator approximation (nonlinear) polyatomic molecules exhibit $3N-6$ normal coordinates along which they vibrate. Transitions occur, as shown by the solid arrows in Figure 1.11(a), within each energy ladder, and transitions between different vibrational coordinates do not occur. As discussed earlier, the transition will originate in all likelihood from the vibrational ground states of each normal coordinate, because they are, by far, the most populated states at room temperature.

Thus, within the harmonic oscillator formalism, the vibrational spectrum should consist of $3N-6$ spectral bands, each one associated with the $n=0$ to $n=1$ transition along each normal coordinate. In reality, the situation is much more complicated. Anharmonicity, as discussed earlier for diatomic molecules, reduces the spacing of energy levels and makes the wavefunctions asymmetric with respect to the equilibrium distance position. Thus, not only are there overtones ($\Delta n=\pm 2$) weakly allowed in the spectra of anharmonic, polyatomic molecules (gray arrows in Figure 1.11(b)), but the so-called "combination bands" are weakly allowed as well. These transitions occur between different normal coordinates, for example, the $n=0$ to $n=1$ transition along coordinate Q_1 in Figure 1.11 that occurs at wavenumber $\tilde{\nu}_1$ and the $n=0$ to $n=1$ transition along coordinate Q_2 that occurs at wavenumber $\tilde{\nu}_2$ can interact. Thus, a "combination transition" that occurs at $\tilde{\nu}_1+\tilde{\nu}_2$ may be observed. In addition to combination bands, "difference bands" at $\tilde{\nu}_1-\tilde{\nu}_2$ may be observed as well. Combination and difference bands, generally, are very weak but can be enhanced by Fermi resonance (see Chapter 5) if their frequency is approximately equal to that of a fundamental transition of the same symmetry species. Fermi resonance is a process that mixes both the fundamental and the combination or overtone band and can result in more than $3N-6$ bands in a spectrum.

On the other hand, in highly symmetric molecules, the number of observed bands in a spectrum can be reduced substantially as discussed in Chapter 2. This reduction of observed bands has two causes: first, the transition moment for absorption for highly symmetric moments may be zero, and the transition is not allowed in IR absorption. The symmetric stretching vibration for methane, CH_4, is a typical example: as this mode does not change the dipole transition moment, it is "infrared forbidden," although it is allowed in Raman scattering. This demonstrates that the vibration along the symmetric stretching coordinate certainly does occur, but that this vibration cannot interact with the electromagnetic field to cause absorption. The second reason for reduced number of observed bands in a vibrational spectrum is the possibility of degeneracy. Degenerate vibrations

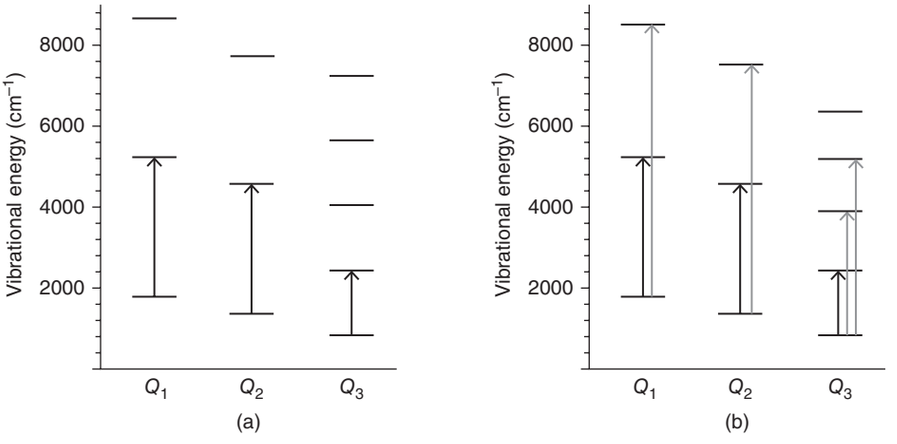

Figure 1.11 *(a) Allowed transitions (solid black arrows) for a polyatomic molecule within the harmonic oscillator approximation. (b) Additional overtone transitions (gray arrows) for an anharmonic polyatomic molecule*

may be visualized as certain vibrational displacements (normal modes) that occur at exactly the same energy. Doubly degenerate (*E* symmetry) and triply degenerate (*T* symmetry) modes, to be discussed in more detail in Chapter 2, will account for two or three degrees of freedom, respectively, and will reduce the number of bands observed in a spectrum.

1.5.5 Isotopic effects: diatomic molecules

The dependence of the vibrational frequency on the reduced mass was discussed earlier for (harmonic) diatomic molecules:

$$\omega = 2\pi\nu = \sqrt{\frac{k}{m}} \tag{1.27}$$

with the reduced mass given by

$$m = \frac{m_1 m_2}{m_1 + m_2} \tag{1.25}$$

When one substitutes an H atom in a diatomic molecule, such as HCl by a deuterium atom with a mass of 2.0 amu, and assumes the same potential energy function (force constant), one finds that the vibrational frequency ω is reduced by a factor of about 1.4 or $\sqrt{2}$. This statement is discussed in detail next. First of all, the assumption that the potential energy curve (see Figure 1.6) is independent of the mass makes sense because the additional neutron in the nucleus of deuterium, as compared to hydrogen, is not expected to influence the potential the electron pair binding the two atoms together.

Second, a comparison of the reduced masses of HCl and DCl yields for the ^{35}Cl isotopic species:

$$m_{\mathrm{HCl}} = \frac{1 \times 35}{1 + 35} = 0.972 \tag{1.106}$$

$$m_{\mathrm{DCl}} = \frac{2 \times 35}{2 + 35} = 1.892 \tag{1.107}$$

which allows an estimate of the vibrational frequency of DCl as follows:

$$\frac{\nu_{\mathrm{DCl}}}{\nu_{\mathrm{HCl}}} = \frac{\sqrt{\frac{k}{m_{\mathrm{DCl}}}}}{\sqrt{\frac{k}{m_{\mathrm{HCl}}}}} = \sqrt{\frac{m_{\mathrm{HCl}}}{m_{\mathrm{DCl}}}} = \sqrt{\frac{0.972}{1.892}} = 0.717 \approx \frac{1}{\sqrt{2}} \tag{1.108}$$

$$\nu_{\mathrm{DCl}} = 2990 \times 0.717 = 2144\ \mathrm{cm}^{-1} \tag{1.109}$$

This frequency agrees reasonably well with the observed frequency of 2091 cm^{-1}. The transition wavenumber for HCl, in Eq. 1.109, was introduced earlier (see Eqs. 1.103 and 1.104).

Third, the lowered vibrational frequency of the isotopic species causes the ground-state vibrational energy, E_0, to be at 1045 cm^{-1} *vs* 1495 cm^{-1} (for HCl). As for anharmonic species, the vibrational potential energy function is slightly asymmetric (see Figure 1.6) and the DCl species is at a lower energy level than HCl, its bond length is slightly lower and its dissociation energy is higher than that of HCl. These findings account for the kinetic isotope effect that states that the rates of chemical reactions that involve the exchange of hydrogen in the transition state may be significantly slower for deuterated species.

The arguments presented here for a diatomic molecule can be applied to polyatomic molecules, such as chloroform and deuterochloroform ($HCCl_3$ and $DCCl_3$, see Section 2.6) by assuming that the —CCl_3 moiety, to a first approximation, acts as a pseudo-atom of mass 117, and that its vibrations do not couple strongly with the C—H stretching vibration. This rather crude assumption actually produces reasonably good results. Similarly, a deuterated methyl group, —CD_3, exhibits stretching vibrations that are shifted by approximately a factor of 0.71 as compared to a —CH_3 group (see Section 2.6).

1.6 Basic infrared and Raman spectroscopies

In this section, the fundamental principles of IR and Raman spectroscopies, the two most common modalities of vibrational spectroscopy, are explored. Both these techniques are commonplace in research and teaching laboratories and in quality control in industrial environments. Furthermore, these techniques can now be found in forensic applications because they both provide highly specific spectral fingerprints for the identification of contraband materials. In this section, a very basic view of the two techniques is presented, emphasizing the differences and commonalities between the methods and introducing some of the instrumental aspects. A more detailed view is presented after the discussion of symmetry and group theoretical aspects (Chapter 2) in Chapters 3 and 4.

1.6.1 Infrared absorption spectroscopy

As pointed out in Section 1.5, IR absorption spectra are observed mostly between the ground and first excited vibrational states; the transitions observed are dipole-mediated, which implies that the normal coordinate along which the transition occurs must change at least one of the Cartesian components of the electric dipole moment (see Chapter 2) for a transition to take place. As the name implies, this modality is observed in "transmission" mode (and converted into absorbance units, see below) where the attenuation (absorption) of IR radiation passing through the sample is observed. According to the condition that the photon energy must match the energy difference between the vibrational states, that is,

$$\Delta E_{\text{molecule}} = E_{\text{photon}} \tag{1.90}$$

only certain "colors" (wavelengths or wavenumbers) of the exciting light will be absorbed, and a spectrum is obtained that is lacking these "colors," or has these colors at reduced intensities. Thus, IR absorption spectroscopy is observed by ratioing the intensity of the incident IR radiation with the intensity of the light transmitted by the sample. This ratio is generally referred as the "transmittance" of the sample. Thus, obtaining an IR absorption spectrum really involves the collection of two separate spectral patterns, the "background" and the "sample" spectra. A typical background spectrum is shown in Figure 1.12(a). Given that the output of an IR source as well as the response of an IR detector generally vary gently with wavelength, the intensity variations in the background spectrum may appear as a surprise. The overall shape of this curve depends on the intensity distribution of the source, typically a black-body (*cf.* Chapter 3) operating at temperatures between 1200 and 2000 °C. The radiance of such a source increases toward the visible part of the electromagnetic spectrum and, therefore, should be higher at 4000 cm^{-1} than at 1000 cm^{-1}. However, the detector used to collect the background spectrum shown in Figure 1.12 was a typical cryogenic HgCdTe detector (see Chapter 3). The peak sensitivity of such a detector occurs at about 1200 cm^{-1} and gradually decreases toward higher wavenumber. Thus, the overall shape of the background curve depends on the source emission profile convoluted with the detector sensitivity profile and the response of the optical components in the beam path, and it is represented in Figure 1.12(a). Frequently, sharp spectral features are observed in the background spectrum between 1300 and 1900 cm^{-1}, and between 3600 and 3900 cm^{-1}; these features are rot-vibrational transitions of atmospheric water vapor, which can present a major problem (see Section 5.4.3). Similarly, a broader feature around 2300 cm^{-1} is due to the rot-vibrational spectrum of carbon dioxide. Both these spectral interferences are discussed later.

In principle, the background spectral features will disappear from the observed IR spectra because of the ratioing between sample and background spectra. However, if there are any changes in the concentration of water and CO_2 between the time the sample and background spectra were collected, their spectral features may be contained in the observed IR spectra of the sample. Thus, it is advantageous to purge the entire instrument

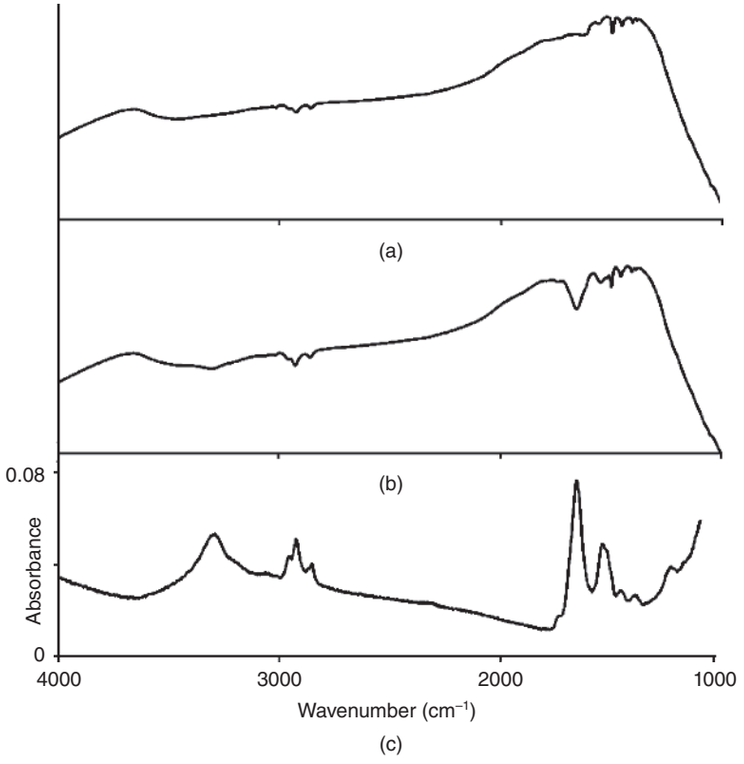

Figure 1.12 *Example of background, sample, and absorption spectra in infrared spectroscopy. (a) Single-beam background spectrum measured in transmission of a single CaF_2 window. The weak features around 2900 and 1500 cm^{-1} are due to a coating on the beam splitter. Note the absence of water vapor and CO_2 features in a well-purged instrument. (b) Single-beam sample spectrum. The intensity scale in (a) and (b) is in arbitrary units. (c) Absorbance spectrum calculated from traces (a) and (b) according to Eq. 1.111. The upward slope of the absorbance spectrum below 1100 cm^{-1} is due to the CaF_2 cutoff*

with dry, CO_2-free air for high-quality data acquisition. Once the background spectrum has been collected, the sample is inserted into the optical beam, and the sample transmission spectrum is collected.

Samples for IR spectroscopy can be gaseous, liquid, or solid. Detailed sampling methodologies are presented in Chapter 3; for the time being, the collection of IR spectra for a neat liquid is discussed. Molar extinction coefficients (see below) for vibrational transitions typically are in the range 10–1000 L $(mol\ cm)^{-1}$, which requires that neat liquids be measured as thin layers, typically between 10 and 100 μm thick. To this end, the sample is introduced into a liquid cell made of IR transparent windows separated by a spacer of appropriate thickness. The choice of IR transparent window materials is by no means trivial. While ultraviolet–visible (UV–vis) spectroscopy can be carried out in glass or quartz cells, both these materials do not transmit mid-IR radiation and are unsuitable for us in IR spectroscopy. This is because both materials contain Si—O bonds whose vibrations occur, like those of most other molecules, in the mid-IR spectral region. Thus, materials for windows (and, for that matter, for all other optical components such as lenses or substrates) must be found that are devoid of molecular bonds. This leaves a fairly restricted choice based mostly on ionic salts such as NaCl, KCl, KBr, AgCl, AgBr, and CaF_2 and a few more esoteric materials. Many of these window materials exhibit

rather undesirable properties, such as solvent incompatibility, toxicity, sensitivity to visible light, restricted optical transmission, or high refractive index. Table 3.2 summarizes many of the window materials commonly used in IR spectroscopy and their optical properties. In most IR spectrometers, the beam diameter at the sample is about 3–4 mm; combined with the required sample thickness (path length), the necessary sample volume is typically about 1 mm^3 or 1 μL.

A typical "sample" spectrum is shown in Figure 1.12(b). The changes between the background trace, $I_0(\tilde{\nu})$, and the sample trace, $I(\tilde{\nu})$, are readily apparent. Subsequently, the two traces are ratioed to yield the transmittance spectrum T as a function of wavenumber (or wavelength):

$$T(\tilde{\nu}) = \frac{I(\tilde{\nu})}{I_0(\tilde{\nu})} \tag{1.110}$$

The ordinate values for the transmittance spectrum vary between 0 and 1. Often, the transmittance is multiplied by 100, and the spectra are reported in "percent transmission" ordinate values.

Taken the negative (decadic) logarithm of the transmittance, the "absorbance" $A(\tilde{\nu})$ of the sample as a function of wavenumber or (wavelength) is obtained:

$$A(\tilde{\nu}) = -\log_{10} T(\tilde{\nu}) = -\log_{10} \frac{I(\tilde{\nu})}{I_0(\tilde{\nu})} \tag{1.111}$$

The absorbance is a unitless (logarithmic) quantity and often is equated to the optical density (OD). Thus, it is common to find the absorbance reported using expressions such as "... the sample had an absorbance of 1.5 OD units." As absorbance is a logarithmic quantity, one absorbance unit corresponds to 90% of all photons incident on the sample being absorbed, whereas two absorbance units correspond to 99% of all photons being absorbed. The absorbance spectrum obtained by converting the two traces shown in Figure 1.12(a) and (b) according to Eq. 1.111 is shown in Figure 1.12(c).

An absorbance spectrum is an experimental manifestation of the interaction of light with the molecular transitions in the sample. It can be related to the theoretical quantities derived in Section 1.5 according to the Lambert–Beer equation:

$$A(\tilde{\nu}) = \epsilon(\tilde{\nu})\, C\, l \tag{1.112}$$

where ε $(\tilde{\nu})$ is the molar extinction coefficient (with units of $(\mathrm{L\,mol^{-1}\,cm^{-1}})$), C the concentration of the sample $(\mathrm{mol\,L^{-1}})$, and l the length the light beam travels through the sample (the path length or thickness of the sample), expressed in centimeters. As discussed earlier, the sample thickness is typically between 10 and 100 μm or 0.001 and 0.01 cm. The molar extinction coefficient is related directly to the transition moment according to

$$D_{01} \propto \langle \psi_1 |\, \mu | \psi_0 \rangle^2 = \frac{1}{\tilde{\nu}_0} \int_{\text{band}} \varepsilon(\tilde{\nu})\, d\tilde{\nu} \tag{1.113}$$

Here, D_{01} is known as the dipole strength of the transition, $\tilde{\nu}_0$ is the center of the band position, and the integration is over the entire band profile that is assumed to follow Gaussian (Eq. 1.114), Lorentzian (Eq. 1.115), or mixed Gaussian/Lorentzian profiles, shown in Figure 1.13. These band envelopes are given by

$$f(x) = Ie^{-\frac{(x-x_0)^2}{2a}} \tag{1.114}$$

for Gaussian and

$$f(x) = I\, \frac{2a}{(x - x_0)^2 - a^2} \tag{1.115}$$

for Lorentzian bands.

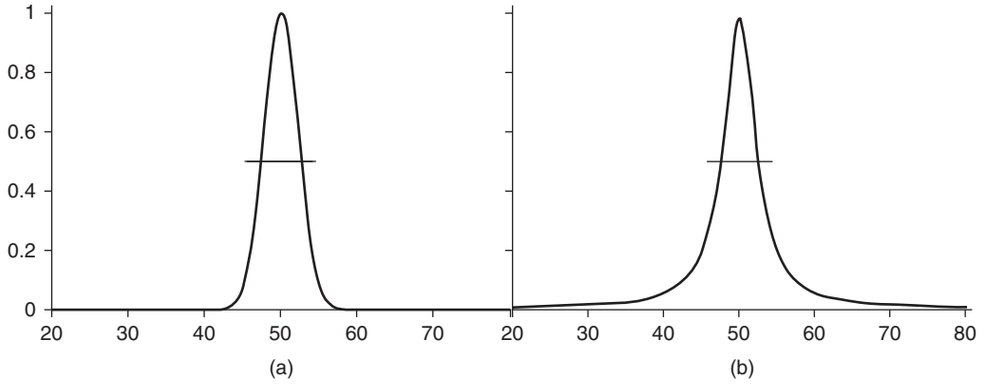

Figure 1.13 *Gaussian (a) and Lorentzian (b) line profiles. Note that the areas under the line profiles are unequal; however, both bands have a full width "*a*" at half maximum (FWHM) of 5 and an intensity* I = *1.0*

Before about 1970, nearly all IR spectroscopy was carried out using dispersive instruments; that is, spectrometers that incorporated a monochromator to separate the broadband radiation from the IR source into narrow wavenumber bands that were tuned in time to expose the sample to the different IR "colors." These monochromators utilized gratings or prisms to disperse the light and slits of appropriate widths to select an appropriate wavenumber band to irradiate the sample. As only one spectral element (band) was sampled at a time, acquisition of spectral data took minutes to hours. These instruments generally operated in "double-beam" mode were a chopper alternatingly directed the beam of light through a reference (background) and sample optical path. Such, the two spectra shown in Figure 1.12(a) and (b) were acquired quasi-simultaneously and ratioed by analog electronics.

Since the advent of laboratory minicomputers, such as the PDP8 by the Digital Equipment Corporation in the mid-1970s, or personal computers in the 1980s, nearly all IR spectroscopy is being carried out by Fourier transform methods, and the techniques is referred to Fourier transform infrared (FTIR) spectroscopy. In FTIR, the light is not encoded sequentially into different colors by a monochromator but simultaneously by an interferometer to yield an interferogram. Fourier transform of the interferogram reveals the IR spectrum. In general, FTIR spectrometers are not operated in dual-beam mode; thus, the sample and background spectra shown in Figure 1.12 were collected consecutively. A more detailed discussion of the principles of the instrumentation, data acquisition, and many other aspects of IR spectroscopy are presented in Chapter 3.

1.6.2 Raman (scattering) spectroscopy

In Raman scattering, a totally different mechanism of excitation from the ground state to the excited state occurs, which is discussed in more detail in Chapter 4. Here, a qualitative approach is taken to introduce the differences and similarities between Raman and IR spectroscopies.

Although the vibrational excitation results in the same final state in both Raman and IR spectroscopies, the excitation process is a result of a two-photon process in the former: a "momentary absorption" into a "virtual state" of a photon with much higher energy than required for the vibrational transition, accompanied by a simultaneous re-emission (scattering) of a photon from the virtual state into either the ground vibrational state (Rayleigh scattering) or the vibrationally excited state (Stokes Raman scattering). These processes are depicted schematically in Figure 1.14(a). Whereas the Rayleigh-scattered photon has the same energy as the incident laser photon, the (inelastically) scattered Raman photon has lost part of its energy to the molecular

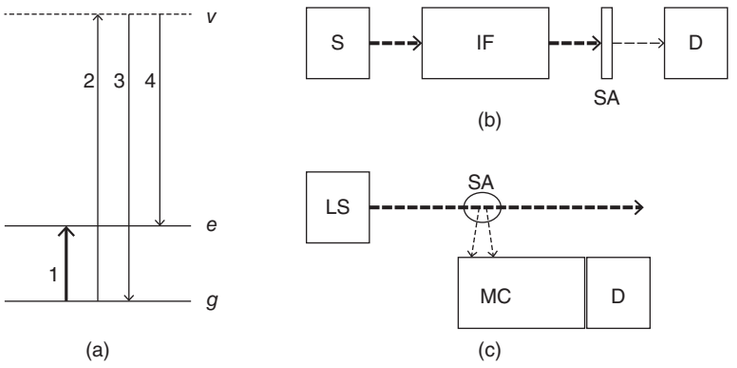

Figure 1.14 *(a) Comparison of infrared absorption and Raman process. g: ground vibrational state, e: excited vibrational state, and v: virtual state. 1: infrared transition, 2: momentary absorption of (laser) photon into virtual state, 3: Rayleigh scattering, and 4: Stokes Raman scattering. (b) Schematic of infrared absorption experiment: S: source, IF: interferometer, SA: sample, and D: detector. The dashed arrows represent the light path. (c) Schematic of Raman scattering experiment. LS: laser source, SA: sample, MC: monochromator, and D: detector*

system, and, therefore, appears at a red-shifted (lower energy) frequency as compared to the incident photon. A comparison of the processes occurring in IR and Raman spectroscopies is shown in Figure 1.14, along with schematic representations of the instruments used for their observation. A third scattering possibility, known as anti-Stokes Raman scattering, is introduced in Chapter 4.

Both Rayleigh and Raman scatterings are extremely weak processes: the Rayleigh scattering process occurs with a likelihood of about 1 in a million; the (nonresonant) spontaneous Stokes Raman process with a likelihood of about $1{:}10^{10}$ to $1{:}10^{12}$, whereas in IR spectroscopy, the chance of a photon incident on the sample to be absorbed can be quite high (in a band with an intensity of one absorbance unit, 90% of the photons are being absorbed). Thus, effective excitation of Stokes Raman spectra is possible only with laser sources that can produce 10^{15}–10^{18} visible photons per second. This fact explains why Raman spectroscopy was a field of very limited applicability before the availability of commercial lasers that occurred in the mid-1970s. Both FTIR and Raman spectroscopies experienced a rebirth at that point in time, and a still ongoing exponential growth ever since.

Raman-scattered light can be collected along the propagation direction of the laser (0° scattering), perpendicular to the propagation direction (90° scattering), or in backscattering (180° scattering). As explained in Chapter 4, 90° scattering was the preferred way to collect Raman spectra until holographic cut-off filters were commercially available to separate the Rayleigh scattering from the Raman scattering; thus, the 90° scattering geometry used prior to this point in time will be used here to explain the collection of Raman spectra data. Similar to fluorescence spectra that are often observed at right angle, the light emitted (scattered) by the sample is collected through a low *f*-number (large aperture) lens and focused onto the entrance slit of a monochromator that separates it into its different color components. For the observation of Raman spectra, the collected light also contains the Rayleigh scattering at the laser wavelength, as well as the much weaker and red-shifted Raman scattering. Within the monochromator, the light is dispersed spatially by a grating, and the intensities of the different, red-shifted Raman components are measured by a solid-state detector such as a charge-coupled device (CCD) camera. Using high-quality detectors and excitation powers between 10 and 100 mW, a good quality Raman spectrum can be collected in about 1 s over the entire spectral range, from about 300 to 3600 cm^{-1} shift from the Rayleigh line.

While IR spectroscopy is caused by direct absorption of a photon to promote the molecule into a vibrationally excited state and requires a change of the dipole moment along a vibrational coordinate, Raman spectra require the polarizability of a molecule to change along a vibrational coordinate. The polarizability of a molecule is its response to the incident radiation far from an electronic transition. This can be visualized as follows. In a clear, colorless liquid, for example, there are no electronic transitions between about 400 and 750 nm, or about 25,000 and 13,000 cm^{-1} (hence the material is colorless). Visible electromagnetic radiation, however, still can interact with the molecule by setting in motion the electron clouds, particularly those in multiple bonds. This phenomenon is referred to as molecular polarization, mediated by the polarizability. Thus, even far from resonance, the light causes an induced dipole moment μ_{ind}, which is proportional to the field strength E of the electromagnetic field:

$$\mu_{\text{ind}} = \alpha E \tag{1.116}$$

where the proportionality constant α is referred to as the polarizability. As both the induced dipole moment and the electric field are vectors, the polarizability is actually a tensor. This is an important aspect that is discussed in detail in Chapter 4.

This polarizability varies as the molecule oscillates along its normal coordinates, Q_k, because the polarizability (i.e., the ease with which electrons can be moved around) depends very much on the nuclear coordinates and thereby on the vibrational modes of the molecule. Thus, one may expand the polarizability in a Taylor series about the equilibrium position according to

$$\alpha = \alpha_0 + \left(\frac{\partial \alpha}{\partial Q_k}\right) Q_k \cos(\omega_k t) + \cdots \tag{1.117}$$

where ω_k is the vibrational frequency of normal mode Q_k.

As the exciting electric field of the incident laser radiation can be represented by

$$E = E_0 \cos(\omega_L t) \tag{1.118}$$

and as the molecule modulates the polarizability according to Eq. 1.117, it is obvious that the induced dipole moment emits radiation that contains the product of the two cosine functions that is, according to a well-known trigonometric identity

$$\cos(\omega_L t)\cos(\omega_k t) = \frac{1}{2}[\cos(\omega_L + \omega_k)t + \cos(\omega_L - \omega_k)t] \tag{1.119}$$

The beat frequencies $\omega_L + \omega_k$ and $\omega_L - \omega_k$ are the aforementioned anti-Stokes and Stokes Raman frequencies, respectively. Thus, a simple, classical description of the (off-resonance) interaction of light with a polarizable molecular system can explain some aspects of Raman scattering.

One important aspect of Raman spectroscopy is that the scattered photon generally still is a visible photon. If laser radiation at 488 nm wavelength or 20,491 cm^{-1} (the strong, blue laser emission of an Argon ion laser) is scattered from a molecule that has one vibrational mode, such as CO (with a stretching wavenumber of $\tilde{\nu} = 2145\ cm^{-1}$), the Stokes-scattered photon occurs at $20{,}491 - 2145 = 18{,}346\ cm^{-1}$ or 545 nm, which is a green, visible photon. If the sample was illuminated by the output of a He—Ne laser (632.8 nm or 15,803 cm^{-1}), the scattered photon would occur at $15{,}803 - 2145 = 13{,}658\ cm^{-1}$ or 732 nm, which is at the end of the visible (red) range of the spectrum. Visible light is more easily detected and requires no special optical materials; thus, one of the big advantages of Raman spectroscopy is the use of visible optical detectors, and optical components. This example also shows that the incident photon interacts with the sample regardless of its color: blue and red photons equally create their own virtual states, although the blue photons are scattered with much higher efficiency.

In both IR and Raman spectroscopies, the observed spectrum of CO should consist of one single band at $2145\,cm^{-1}$; however, in gaseous CO, a more complex spectrum that includes rot-vibrational transitions is observed (see Chapter 5).

1.7 Concluding remarks

In the preceding sections, the classical and quantum mechanical formulation of molecular vibrations was reviewed. This review introduced the concept of normal modes of vibration, which is based strictly on a classical mechanical model. In order to explain the observed vibrational spectra, a transition to quantum mechanical models needs to be made. However, these models also invoke the concept of normal coordinates, because the observed transitions are associated with the normal modes of vibration. This description explains the vibrational (absorption or emission) spectra that consist of spectral "bands" at given frequencies. Each of these absorption bands corresponds to a transition along one normal coordinate.

Thus, at least two pieces of information may be extracted from a spectral band: its position (frequency, wavelength, or wavenumber) and intensity. The intensities of each transition are determined by their transition moments, whereas the frequencies are determined by the energy eigenvalues of the vibrational Hamiltonian (Eq. 1.64) that are based on the energy eigenvalues of the "mass-and-spring" secular determinant (Eq. 1.34).

The square of the transition moment is the actual observable in IR absorption spectroscopy: the integrated intensity of an absorption band is the dipole strength D of a transition, which can be determined experimentally as the area under an IR band, plotted in units of the molar extinction coefficient ϵ *vs.* wavenumber (see Eq. 1.108) and shown in Figure 1.13(a) and (b). Both the intensity and the energy of a transition can be calculated from quantum mechanical principles if the wavefunctions of the system are known to a high degree of accuracy. In fact, *ab initio* quantum mechanical calculations of vibrational frequencies and intensities now are practical for molecules with up to 50 heavy (not hydrogen) atoms (see Chapter 9).

References

1. Wilson, E.B., Decius, J.C., and Cross, P.C. (1955) *Molecular Vibrations: The Theory of Infrared and Raman vibrational Spectra*, McGraw-Hill co., New York
2. Kauzman, W. (1957) *Quantum Chemistry*, Academic Press, New York.
3. Levine, I. (1970) *Quantum Chemistry*, vol. 1 and 2., Allyn & Bacon, Boston.
4. Baierl, P. and Kiefer, W. (1975) Hot band and isotopic structure in the resonance Raman spectra of bromine vapor. *J. Chem. Phys.*, **62**, 306–308.